Supramolecular Materials: Self Organized Nanostructures

S. I. Stupp*, V. LeBonheur, K. Walker, L. S. Li, K. Huggins, M. Keser, and A. Amstutz

Department of Materials Science and Engineering,
Department of Chemistry,
Beckman Institute for Advanced Science and Technology,
and Materials Research Laboratory
University of Illinois at Urbana-Champaign

*To whom correspondence should be addressed

Submitted for publication in *Science*

October 1996

Abstract

We have discovered systems of molecules with the architecture of miniaturized triblock copolymers that self assemble into nanostructures highly regular in size and shape. In the system described here, a mushroom-shaped supramolecular structure of about 200 kilodaltons forms by crystallization of the chemically identical blocks in the system. Interestingly, the supramolecular units self organize into films containing one hundred or more layers stacked in polar arrangement. The polar supramolecular material exhibits spontaneous second harmonic generation from infrared to green photons, and a tape-like character with nonadhesive-hydrophobic and hydrophilic-sticky opposite surfaces. The films also have reasonable shear strength, and adhere tenaciously to glass surfaces on one side only. The regular and finite size of the supramolecular units is believed to be mediated by repulsive forces among some of the segments in the triblock molecules. On the other hand, the polar stacking of the mushroom nanostructures might be the system's organization that optimizes space filling in three dimensions. A large diversity of multifunctional materials could be discovered in solids formed by regular supramolecular units in the range of hundreds of kilodaltons. Such supramolecular materials could impact the technologies of sensors, cell substrates, waveguides, membranes, materials coupling in composite structures, solid lubricants, and catalysts, among others.

REPORT DOCUMENTATION PAGE

Form Approved
OMB No. 0704-0188

1. AGENCY USE ONLY (Leave blank)	2. REPORT DATE	3. REPORT TYPE AND DATES COVERED
	1/21/96	Technical 1/1/96 - 12/31/96

4. TITLE AND SUBTITLE

Supramolecular Materials: Self Organized Nanostructures

5. FUNDING NUMBERS

N00014-96-1-0515

R&T Code: 313x004

Dr. Kenneth J. Wynne

6. AUTHOR(S)

Samuel I. Stupp, Vassou LeBonheur, Kenneth A. Walker, Li-Sheng Li, Kevin E. Huggins, Milan Keser, and Aaron Amstutz

7. PERFORMING ORGANIZATION NAME(S) AND ADDRESS(ES)

Department of Materials Science and Engineering
University of Illinois
1304 W. Green St.
Urbana, IL 61801

8. PERFORMING ORGANIZATION REPORT NUMBER

3

9. SPONSORING/MONITORING AGENCY NAME(S) AND ADDRESS(ES)

Dr. Kenneth J. Wynne
Office of Naval Research
Ballston Commons Tower One, room 503
800 North Quincy St.
Arlington, VA 22217-5660

10. SPONSORING/MONITORING AGENCY REPORT NUMBER

11. SUPPLEMENTARY NOTES

Submitted for publication in Science.

12a. DISTRIBUTION/AVAILABILITY STATEMENT

Reproduction in whole or in part is permitted for any purpose of the United States Government; this document has been approved for public release and sale; its distribution is unlimited.

12b. DISTRIBUTION CODE

13. ABSTRACT *(Maximum 200 words)*

We have discovered systems of molecules with the architecture of miniaturized triblock copolymers that self assemble into nanostructures highly regular in size and shape. In the system described here, a mushroom-shaped supramolecular structure of about 200 kilodaltons forms by crystallization of the chemically identical blocks in the system. Interestingly, the supramolecular units self organize into films containing one hundred or more layers stacked in polar arrangement. The polar supramolecular material exhibits spontaneous second harmonic generation from infrared to green photons, and a tape-like character with nonadhesive-hydrophobic and hydrophilic-sticky opposite surfaces. The films also have reasonable shear strength, and adhere tenaciously to glass surfaces on one side only. The regular and finite size of the supramolecular units is believed to be mediated by repulsive forces among some of the segments in the triblock molecules. On the other hand, the polar stacking of the mushroom nanostructures might be the system's organization that optimizes space filling in three dimensions. A large diversity of multifunctional materials could be discovered in solids formed by regular supramolecular units in the range of hundreds of kilodaltons. Such supramolecular materials could impact the technologies of sensors, cell substrates, waveguides, membranes, materials coupling in composite structures, solid lubricants, and catalysts, among others.

14. SUBJECT TERMS

supramolecular materials, self assembly of adhesives, optical materials, chemically defined surfaces

15. NUMBER OF PAGES

16. PRICE CODE

17. SECURITY CLASSIFICATION OF REPORT	18. SECURITY CLASSIFICATION OF THIS PAGE	19. SECURITY CLASSIFICATION OF ABSTRACT	20. LIMITATION OF ABSTRACT
unclassified	unclassified	unclassified	UL

One of the great challenges for materials science is learning to create supramolecular materials in which the constituent units are nearly identical molecular nanostructures. This will require learning to encode in the structure of simple but functional molecules the thermodynamic factors that control their aggregation into large supramolecular units. If necessary for the control of properties, chemical reactions internal to the units could transform them to shape invariant polymers, and external ones could inter-connect them into stable morphologies. The molecular nanostructures of interest as the constituent of materials may have molar masses in the range of 100 to 1,000 kilodaltons and such units are not currently available as compounds prepared with conventional synthetic chemistry. Thus, the search for supramolecular forms of the units accessed by self assembly is an extremely important goal in materials science. Even though in this work we focus on organic nanostructures, many interesting prospects exist for inorganic as well as organic-inorganic hybrids. We believe that learning to assemble supramolecular units, and the elucidation of rules mediating their macroscopic organization into functional materials is a fascinating prospect for technology. Such synthetic nanostructures, analogous to folded proteins in the definition of chemical sectors, shape, and topography, will be interesting building blocks for materials because they must pack in unique ways to fill space efficiently. Figure 1 shows examples of molecular nanostructures including flat and tubular objects, ellipsoids, parallelepipeds, and a mushroom-shaped object, among others. For simple geometrical shapes such as flat objects, rods, and tubules the three dimensional packing can be easily predicted. As illustrated in figure 2 flat objects such as two-dimensional polymers are likely to stack and form layered structures (1,2), tubules and rods align uniaxially, and identically shaped and sized

nanostructures such as the parallelepipeds are likely to tile into a wide variety of superlattices. The objects shown in figure 1 are under investigation in our laboratory, and the formation of some of them has been observed experimentally (3).

One could envision a large variety of functional materials synthesized with molecular nanostructures. One possibility is the formation of micro- or macroscopic structures made up of stacked plates with surface properties that reflect directly the chemical exterior of flat nanostructures. Another example would be cables or microfibers formed by aligned tubules that could select and direct molecules or ions in space. It is also possible to envision macroscopic objects or lithographically fabricated domains made up of superlattices formed by nanostructures with sensing features. Such features could include cavities or protrusions that present to an external environment huge arrays of binding sites for small or large molecules. Alternatively, similar superlattices may function as membranes since the packing of nanostructures (depending on their shape) could create free volume that is available for the selective flow of liquids or gases. Since materials are structures that need to express their functionality in macroscopic forms, the vision will require understanding not only nanostructure formation by self assembly but also nanostructure packing and networking in three dimensions. In spite of great progress in the field of supramolecular chemistry over the past decade, much remains unknown if one considers the broad spectrum of length scales from molecular aggregates to macroscopic objects.

The field of supramolecular chemistry was pioneered by seminal work in the laboratory of Jean-Marie Lehn, and a lot of this work and that of others have been summarized recently (4). Whitesides and coworkers have also studied a number of systems with the objective of synthesizing well defined nanoscale compounds in the molar mass range of a few kilodaltons (5-7). The self assembly of other similar organic structures through hydrogen bonds has also been studied in the context of dendrimers (8), and polydisperse systems that form liquid cyrstals by hydrogen bonding have been studied by Frechet and co-workers (9,10). Our laboratory has reported on the combined use of self assembly and chemical reaction in chiral monomers to generate two-dimensional polymers (1,2). We have also investigated the formation of nanostructures by self assembly using rodcoil polymers, having a rigid molecular segment covalently attached to a very flexible sequence of isoprene segments (3). In this work we found that rodcoil polymers can self assemble into long strip-like aggregates (close to a micron or more), and a few nanometers in the other dimensions. As the flexible segment of the rodcoil polymer increased in length relative to the rod-like segment, the molecules were found to self assemble into discrete disc-like aggregates such as those shown in figure 1.

Our goal in this work has been to study strategies to create huge numbers of copies of supramolecular units with similar size and shape. As mentioned before, such shape invariant nanostructures could also be considered polymers if their constituent molecules were to be stitched internally at multiple sites with covalent bonds. For reasons that will become more apparent at the end of this article, macroscopic organization of such nanostructures could help us learn what is needed

to develop device-like materials that are created on demand without the use of complex hardware, and also would provide us with abiotic systems to learn about self assembly with the length scales of biological systems. The work reported here describes the self assembly of mushroom-shaped nanostructures using as precursors small molecules with chemical sequences inspired by block copolymer chemistry.

Synthesis

We synthesized molecules with the structure shown below which can be described as miniaturized triblock polymers,

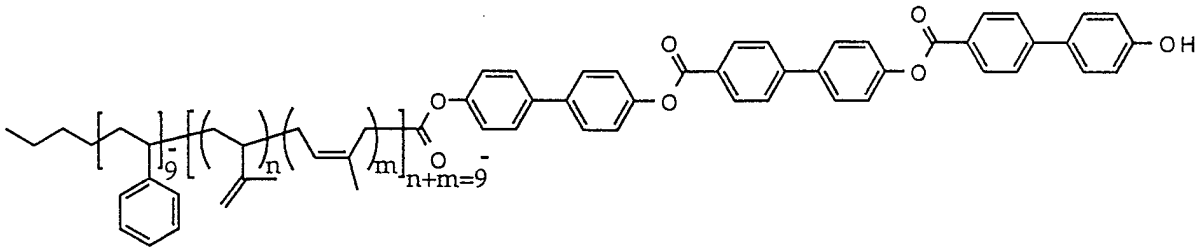

1

A molecular graphics representation of one of these molecules is shown in figure 3. The synthesis starts with the reaction known as living anionic polymerization discovered by Szwarc (11) (using in this case styrene monomer initiated by n-butyl lithium). However, the amount of monomer supplied is only sufficient to create a miniature styrene chain with an average degree of polymerization of 9. A second block of similar average degree of polymerization grows when isoprene is added, acting as an electrophile to the living anions in the reaction medium (12). In a third step, carbon dioxide quenches the isoprenic living anion and installs carboxyl end

groups at the end of the miniature diblock copolymers (13). This carboxyl group can then be used as a junction point to attach the third block by esterification reactions. As shown in scheme 1 (14), the third block is a rigid chemical sequence built by the esterification of **2** and **3**, followed by deprotection at the phenolic terminus and a second esterification of compounds **4** and **5**. The final triblock structure **1** is obtained after a second deprotection of the phenolic terminus. This triblock structure has two aperiodic blocks which are chemically diverse in the system, and one rod-like block identical in all molecules. One terminus of the triblock is a hydrophobic methyl group (from the n-butyl lithium initiator), and the opposite terminus is hydrophilic, consisting of a phenolic group.

One could say the triblock molecules of interest here have "rodcoil" architecture since one segment is a stiff, rod-like chemical sequence which is covalently connected to a more torsionally flexible diblock segment. In solution these diblock sequences would have coil-like conformations. The polydispersity of the triblock molecules ($\overline{M}_w/\overline{M}_n$) measured by gel permeation chromotography is in the range of 1.06 and 1.1. Figure 4 presents a sampling of 20 chemical sequences for the coil diblock to emphasize its structural diversity in the system (15). The styrene block is atactic and is thus a random sequence of meso (m) and racemic (r) diads, the isoprene segment has mostly repeats from 1,4 and 3,4 addition but can also have a trace of 1,2 units (based on nuclear magnetic resonance). Even though both blocks are nonamers on average, the diblock sequences should have a distribution of molar mass which is comparable or slightly narrower than a Poisson distribution (this statement is based on FDI (16) mass spectrometry of short styrene segments). This distribution contributes further to

the structural diversity of the system of triblock molecules. In great contrast, the rod segment is analogous to a chemical compound and it is therefore the common structural element shared by all molecules.

Structure

When thin films of the triblock molecules were cast from chloroform dilute solutions (2-3 mg/ml), we discovered that nearly identical nano-sized aggregates formed as revealed by the electron micrographs in figures 5a and 5b. These electron micrographs were obtained without using any staining compound. Thus, the contrast observed in the micrograph is due exclusively to phase contrast, indicating that part of the structure scatters electrons (dark spots) and is crystalline. This was confirmed by the wide angle electron diffraction pattern shown in figure 6. Since the only segment that could organize into a crystalline lattice is the rod-like segment, the dark regions observed must consist of ordered clusters of the rigid biphenyl ester blocks. The diffraction pattern reveals an a*b* reciprocal lattice plane, indicating that rod segments are oriented normal to the plane of the micrograph. The interesting fact that all dark spots are of similar shape and size indicates that these aggregates must contain about the same number of molecules. The similarity in shape and size is fingerprinted by self organization of the aggregates into a superlattice with periodicities of 70 Å and 66 Å. The images shown in figures 5a and 5b as well as the small angle electron diffraction pattern in figure 7 characterize the superlattice as monoclinic with a characteristic angle of 110° (the aggregates are located at the lattice points of the (001) plane of a monoclinic unit cell). Many small domains of the monoclinic superlattice are visible in the images of figure 5.

Crystallization of the identical rod-like segments in the miniature triblock polymer must exclude the chemically diverse oligostyryl and oligoisoprene blocks. In our view, the chemical aperiodicity and diversity of these two segments in the triblock population of molecules is an extremely important factor in the type of self assembly observed in this system. These two segments frustrate the global ordering of the system, thus preventing the usual formation of a three dimensional organic crystal. Thus, the disruption of chemical regularity in two of the blocks in each triblock molecule predisposes the system to form finite aggregates. The oligoisoprene segment is extremely flexible, given that polyisoprene is a rubber at room temperature, and also has a small cross sectional area relative to the styrene segment. The isoprene blocks therefore serve as a structural buffer that can stretch and pack to accommodate the density of the crystallizing segments. The biphenyl ester segments have of course an extremely high tendency to aggregate and order through π-π overlaps. This is failry evident in the insolubility of a compound containing only the rod-like segment of the triblock structure. Also, polymers with similar structures in their chemical repeats have extremely high melting points if they fuse at all before reaching the regime of chemical decomposition. The oligostyrene segments have a fairly large cross section because of their phenyl substitution of the carbon backbone. Thus, as oligostyrene segments try to accommodate the nanocrystal's density, they will no doubt experience strong hard core repulsive forces (we return to this point at the end of the manuscript). These repulsive forces could balance the favorable association of aromatic blocks and prevent the infinite aggregation of triblock molecules. In addition to the usual entropic penalties linked to molecular aggregation (i.e. translational), an additional entropic loss in this case could be linked to stretching of the flexible

isoprene strands in order to accomodate rod-rod interactions. Finite aggregation into nanostructures reduces this penalty because it allows coils to splay at the periphery of the supramolecular unit. Finite aggregation may also prevent the entropically unfavorable vitrification of packed coil segments exposed to repulsive interactions.

Fourier transform infrared spectroscopy indicates that annealing of the films at 250°C for 2 hours leads to crosslinking of the triblock molecules by reaction among isoprene segments, consuming about 40% of their double bonds. This reaction, which has a well defined exothermic signature in differential scanning calorimetry scans (with an onset temperature of 300°C), does not lead to the formation of a three dimensional gel. Once crosslinking occurs, the samples remain thermoplastic and a birefringent melt is observed at 250°C (17). Isotropization of the birefringent fluid is never observed prior to chemical decomposition above 400°C. Following crosslinking, the crystalline order of rod segments in the self assembled aggregates improves as revealed by the electron diffraction pattern shown in figure 8. We do not know at this time if the reaction is confined within the discrete supramolecular units, transforming them to covalent polymers. However, it is clear that a three dimensional network does not form as a result of crosslinking and the system remains a *nanostructured material.*

Solution cast films coated with carbon on one side and placed on gold grids were embedded in epoxy for ultramicrotomy. These films were close to a micron in thickness and prior to the embedding procedure had been annealed at 250°C for two hours, and also exposed to OsO_4 vapors for 15 hours. OsO_4 was used as a standard

staining procedure for the remaining double bonds in isoprene segments in order to improve contrast in electron microscopy. After staining, the gold-organic-carbon sandwich was microtomed with a diamond knife into sections 50 to 100 nanometers thick. Gold was necessary for this procedure because of its low hardness, and also the flanking of the organic film by gold and carbon on opposite surfaces offered an excellent tracer to find it under the electron beam. Also, ultramicrotoming of the thin films is possible only after the crosslinking reaction which increases the mechanical integrity of the film. After crosslinking we also find that atomic force microscopy tips do not mechanically damage the film's surface. Interestingly, we discovered that sections from films approximately one cm^2 in area and nearly one micron in thickness were made up of many layers all oriented with a common surface normal. The characteristic period of the layers with a common stacking direction was found to be about 70 Å, consisting of one dark and one light band with thicknesses of 30 Å and 40 Å, respectively. Figure 9 shows the transmission electron micrograph of one of the ultramicrotomed sections at two different magnifications, as well as a fourier filtered image (18) revealing very clearly the periodicity and orientation of the layers. This Fourier filtered image was obtained using only the meridional intensity in the fourier transform to highlight the layered nature of the self organized film. However, if a fourier transform of the image is obtained one observes also some equatorial intensity suggesting that layers are not continuous but are instead made up of nanostructures. When the image is regenerated from Fourier transform that includes also non-meridional intensity, one does indeed observe that layers are made up of discrete nanostructures (see figure 10). This suggests that crosslinking reactions may indeed be confined within the volume of supramolecular units.

The electron micrograph of the ultramicrotomed films reveals information on how the nanostructures might be stacked to form the macroscopic films. We interpret the dark and light bands as regions containing the crystalline rods and the amorphous coil segments, respectively. This interpretation is based on two facts. The thickness of dark bands is roughly equivalent to the length of one extended rod segment, and secondly we know that a rather strong phase contrast results from the crystallization of rod blocks alone as demonstrated by the micrographs of unstained samples in figure 5. The thicker light band, on the other hand, could correspond to partly splayed diblock segments of styrene and isoprene structural units. The OsO_4 stain did not seem to provide any additional contrast, and this may be due to crosslinking among isoprene units during annealing. Additional evidence for a characteristic periodicity in films equivalent to one triblock molecule was offered by electron microscopy of platinum shadowed samples. These shadowed samples were imaged at their edges where the films were thinnest. The distinct steps or terraces observed in the films all had dimensions definitely under 100 Å, thus suggesting the nanostructures self organize as monolayers and not as bilayers. However, one must consider the possibility that interdigitation of both rods and coils occurs in these supramolecular units. The interdigitation of rods would be thermodynamically logical since it would create more volume for the flexible diblock segments to explore conformational space. However, the interdigitation of both rod and diblock coil segments may not be favorable given the large cross section of styrene blocks. We examine this question below using packing energy calculations with a force field for the various blocks in the molecules.

In an effort to understand further the packing of triblock molecules in the system studied we have calculated cluster energies for coil and rod blocks using the Tripos force field (19). The packing of diblock segments containing the styrene and isoprene sequences results in repulsive interactions which are stronger when the segments are antiparallel. That is, based on these calculations interdigitation of coils would not be favorable. On the other hand, the energies are much lower when diblock coils are packed in a nanophase separated state, that is with pure styrene and pure isoprene regions. If diblock coils cannot interdigitate, the interpretation of TEM images must be that molecules are assembled into nanostructures that are one molecule thick with nanophase separation of all three blocks. Furthermore, in order for this type of aggregate to generate an image with layers of alternating light and dark bands, the nanostructures must be stacked in polar fashion and not antiparallel to each other within the layers. As mentioned above, interdigitation of rod segments would be entropically favorable for the more flexible segments grafted to the rod segment. However, this type of packing with non-interdigitated coils would have revealed a thicker light band than the one observed (two fully extended average diblocks would measure about 120 Å and the light band is only 40 Å).

Based on the wide angle diffraction pattern of figure 6, the rod-like segments are packed into an orthorhombic unit cell with lattice parameters equal to 5.4 Å and 8.2 Å. Using these unit cell parameters, as well as the cross section and thickness of nanostructures observed in TEM images, we estimate there are approximately 100 molecules in each nanostructure. The supramolecular units would then have a molar mass of approximately 200 kilodaltons. Also, the monoclinic (as opposed to

hexagonal or cubic) nature of the superlattice suggests the supramolecular aggregates have cross sections that are more rectangular than circular in shape. Based on data presented so far, we are led to to the heuristic model of the nanostructure shown in figure 11 which envisions it as a mushroom-like aggregate of about 100 triblock molecules. In this mushroom aggregate, the chemically aperiodic and structurally diverse coil segments are excluded from the crystalline sector formed by identical rod segments.

The model in figure 12 envisions the one micron thick and one cm^2 area films prepared in our laboratory as the layered assembly of trillions of mushroom-shaped nanostructures. The main point made by the schematic representation in figure 12 is the existence of polar order in the layered stacking of the nanostructures. The TEM images of single layers of nanostructures reveal the presence of monoclinic superlattice domains within one layer. We do not know, however, if the mushrooms organize with three dimensional order or if the stacking is uncorrelated through the layers. In other more symmetric molecular nanostructures studied by our laboratory, three dimensional order was observed across several layers (20), and so this possibility cannot be ruled out at this time. Even if a stacking order were to exist, we would expect a given concentration of stacking faults and point defects as is common in most materials.

Properties

Surface properties

We measured contact angles made by water droplets on the surfaces of cast films. These films were cast from chloroform solutions on a water surface, picked up on glass slides, and dried thoroughly under argon. With perfect reproducibility in a very large number of experiments, the top surfaces of these films were always highly hydrophobic and contact angles for water of approximately of 95° were observed. When the films were inverted prior to complete drying using adhesive tape, and dried thoroughly under argon, the contact angles observed for water were always low indicating the formation of a hydrophilic surface. The contrasting hydrophobic-hydrophilic character on opposite surfaces of these films was always observed without requiring any long annealing period after solvent evaporation. This is in contrast to the long annealing periods (hours or days) often required to observe contrasting surface properties in films of block copolymers which may contain hydrophobic backbones and hydrophilic end groups after being cast on polar surfaces (21). The observed surface behavior of films would be consistent but does not prove the formation of polar films by self organization of the nanostructures. Water droplets on opposite surfaces of the supramolecular film are shown in the photographs of figure 13.

Adhesion and Mechanical Properties

Films cast on glass in which the supramolecular units had been internally crosslinked adhere tenaciously to the substrate. According to contact angle data, the film's surface in contact with glass is highly hydrophilic and must therefore expose the phenolic groups of rod segments. Tenacious adhesion to glass could then be related to hydrogen bonding between the substrate and the stems of the mushroom nanostructures. The strong adhesion at the glass-film interface is clearly revealed by

the response of a sample immersed in concentrated hydrofluoric acid (HF). HF is a solvent for glass and dilute aqueous solutions are used routinely in experimental procedures to lift organic films cast on glass. We found that films could not be lifted from glass surfaces even at HF concentrations of 8.6M which visibly etch the glass, producing cracks and pits throughout its surface. This is illustrated in the graph of figure 14, plotting the time elapsed before the glass substrate fractures as a function of acid molarity without ever releasing the nanostructured film. In contrast, a plot in figure 14 shows that films of poly(vinyl phenol) cast on glass detach from the substrate after a period of time which depends on HF molarity. Poly(vinyl phenol) is an interesting conrol since the side chains of repeats in this amorphous polymer are identical to the termini of rod segments in the supramolecular units. The phenolic groups are the ones likely to interact with glass by hydrogen bonding in both cases, but their attachment to the substrate as bundles formed by internally connected supramolecular units must be more effective for adhesion. Finally, two films fused between glass surfaces exhibit a shear strength equal to 1.22 MPa, approximately twice that observed for a film of poly(vinyl phenol) films of comparable thickness (0.53 MPa). It is interesting that the layered supramolecular film, without the benefit of extensive chain entanglements, exhibits a higher adhesive strength than poly(vinyl phenol).

Nonlinear optics

The polar film envisioned in the schematic of figure 12 should not have a center of inversion and could therefore exhibit dipolar second order nonlinear optical activity without requiring electrical poling. Dipolar second order effects would be forbidden in centrosymmetric media, and would only be observed as a result of broken symmetry at

the surface of the film (this is likely to happen in very thin films). We measured the second order activity of films cast from solution on glass substrates and, interestingly, discovered that frequency doubling of an infrared laser beam at 1064 nm is indeed observed well above any possible noise levels in the experiment (22). A simplified schematic of the sample orientation relative to the incident polarization of the beam is shown in Figure 15. The curve in figure 16 shows how the intensity of the second harmonic signal changes at different film surface positions of the incident laser beam. Variations in the intensity of the signal as a function of surface position on the film reflect variations in thickness of the cast film, and this was verified with profilometer scans (see figure 17). Furthermore, we averaged the second harmonic signal on spots varying in thickness (each point representing the average of 1,000 pulses) and have plotted these data in figure 18. The correlation of second harmonic intensity with film thickness is indicative of bulk polar structure in the macroscopic supramolecular film as opposed to just broken symmetry at its surfaces.

In an attempt to verify the origin of the second harmonic signal, measurements were taken using *p*-polarized light as the sample was rotated at 5° intervals about an axis in the plane of the film. These measurements revealed a significant increase in intensity of the second harmonic signal with rotation. This indicates that the conjugated rod segments normal to the glass substrate must contribute to the signal. Furthermore, when using a polarization of the incident beam normal to that in the schematic drawing of figure 15 (*s*-polarization) essentially no signal was observed. This again is expected if the nonlinear optical signal is associated with the rod-like segments oriented normal to the plane of the film. The second harmonic signals were

observed in both annealed and unannealed films, indicating the origin of noncentrosymmetry is the self organization of supramolecular units when films are cast from solution. One has to consider the possibility that the observed signal was the result of quadrupolar second harmonic generation which has been observed recently in centrosymmetric films (23-26). However, this phenomenon has been observed in films with higher symmetries than ours such as phthalocyanine films or C_{60} films. The phthalocyanine films investigated had D_{4h} symmetry and were prepared by molecular beam epitaxy techniques. Because of steric factors, we do not believe our system can have complete molecular interdigitation and consequently the necessary symmetries for quadrupolar effects.

Polar Organization

It remains a challenge to understand the origin of polar organization in the supramolecular material studied. Polar order is an extremely useful source of functionality in materials but this fascinating phenomenon is uncommon in nature. Polar structures are linked to properties of materials such as piezoelectricity, pyroelectricity, second order nonlinear optical susceptibility, and ferroelectricity. Ideal polar order achieved with layered nanostructures also offers a strategy to create films much thicker than a monolayer which still have two chemically distinct surfaces regardless of thickness, surface roughness, and erosion of molecular layers (see the schematic representation in figure 19). If shape invariant nanostructures were to stack with polar order, the contrast between opposite surfaces of a film may not only be based on chemical structure but also topography. For example, a macroscopic film could present nano-cavities or protrusions on one surface and an adhesive surface on

its opposite side for adhesion on a substrate. The fundamental reasons for the appearance of polar order in the system studied here remain but we discuss below some factors that could be considered.

Using an empirical force field we have calculated packing energies for different types of clusters, containing units with the chemical structure present in the triblock molecules studied here. The rod segments in this computer model have extended conformations, without kinks or bends along their length. We applied to the rod segments a genetic algorithm developed in our group for conformational energy minimization (27), and found that virtually all of the low energy conformations found for these segments were fully extended. Our program loads copies of a molecule into SYBYL and builds a very dense cluster, relaxes this cluster using the Tripos force field via conjugate gradient minimization, generating as output the cluster's energy (28). The left side of figure 20 shows a cluster of triblock molecules before complete minimization, color coded for energy and pointing to the styrene coils as a site of high repulsive energy. In the fully relaxed cluster (right side of figure 20) the growth of a mushroom-shaped nanostructure is evident since the coil end of the aggregate has a larger cross section than the rod end. Four other types of clusters (each with 13 units) were analyzed with the force field, two contained rod segments only and the other two the coil-like segments of styrene and isoprene, in either parallel (ferro clusters) or anti-parallel arrangement (antiferro clusters) (see figure 21). Figure 22 shows the four types of clusters with their corresponding energies and cross sectional areas per molecule. The force field calculations yield repulsive energies for diblock coil clusters and attractive energies for rod clusters. Interestingly, the most favorable combination

for an aggregate of the triblock molecules is that of parallel arrangement (ferro) of both rod and diblock segments. These rather simple calculations for small clusters point to the formation of an incipient mushroom nanostructure as the most favorable aggregate, as opposed to a dumbell-like or cylindrical nanostructure resulting from partial or complete inter-digitation of segments. Furthermore, the local densities of isoprene sectors in these clusters are the ones that best match the packing densities of rod segments estimated from unit cell parameters obtained with diffraction experiments. Given the small size of the computational cluster relative to the aggregates discovered experimentally, and the empirical nature of the force field we could not possibly attribute any great significance to these results. However, the results are a useful reminder that details of the covalent structure, typically not accounted for in physical theories, could lead to important differences in the packing arrangements of supramolecular aggregates. These differences could determine if macroscopic collections of the clusters express useful properties and may therefore be considered functional materials.

Having addressed the issue of a non-interdigitated cluster, it is also a challenge to understand why polar stacking of nanostructure layers would occur in the macroscopic film, as opposed to apolar stacking of bilayers. We infer that efficient space filling by mushroom-shaped aggregates of molecules may be an important factor. We believe minimization of free volume in these supramolecular films is important because solvent (chloroform) is tenaciously retained even after films are heated to temperatures more than 100°C higher than the solvent's boiling point of 61°C (29). Chloroform is known to hydrogen bond with carbonyl groups (30,31), and

thus could also bond with phenolic and ester bonds in rod segments. At an entropic cost the solvent could fill space not occupied by the nanostructures, thus avoiding the presence of free volume. In this context one may ask if monolayer as opposed to bilayer stacking of the mushroom nanostructures minimizes the volume that needs to be filled by solvent in order to avoid free volume. As depicted schematically by the objects of figure 23, bilayer stacking could certainly create larger pores which may be more difficult to fill with molecularly flexible segments by x,y,z translations of the nanostructures. On the other hand, polar monolayer stacking of the supramolecular units in three dimensions may fill volume more effectively by such translations. The caps of the mushroom nanostructures should be more deformable than the rod stems and therefore have the flexibility to fill space more efficiently. In the case of bilayer stacks, displacements parallel to the layer normal may not be effective at filling space. Thus, macroscopic objects composed of nanostructured bilayers may require for stability the entrapment of larger amounts of solvent in order to avoid free volume.

Our findings encourage the search for multifunctional materials in solids composed of supramolecular units with regular shape and dimension, or mixtures of such units. Our discovery challenges us to find structurally diverse systems of simple molecules that can find energy minima in nanostructures defined by chemical sectors, topographical features, and global shape. Because of the potential for function integration such supramolecular materials could impact the technologies of sensors, cell substrates, waveguides, membranes, materials coupling in composite structures, solid lubricants, and catalysts, among others.

References and Notes

1. S. I. Stupp, S. Son, H. C. Lin, and L. S. Li, *Science*, **259**, 59 (1993).

2. S. I. Stupp, S. Son, X. Hong, L. S. Li, H. C. Lin, and M. Keser, *J. Am. Chem. Soc.*, **117** (19), 5212 (1995).

3. The disc-like structure shown in figure 1 (top view) forms through the interdigitation of rod segments in rodcoil polymers (L. H. Radzilowski and S. I. Stupp, *Macromolecules*, **27** (26), 7747 (1994); L. H. Radzilowski, B. O. Carragher, and S. I. Stupp, *Macromolecules*, in press). The ellipsoid nanostructures shown in figure 1 can form when rodcoil molecules with long coil segments aggregate into bilayer clusters, W. Eck, L. S. Li, and S. I. Stupp, unpublished results.

4. J.-M. Lehn, *Supramolecular Chemistry*, VCH, Weinheim, New York, (1995).

5. G. M. Whitesides, J. P. Mathias, C. T. Seto, *Science*, **254**, 1312 (1991).

6. C. T. Seto, J. P. Mathias, G.M. Whitesides, *J. Amer. Chem. Soc.*, **115**, 1321 (1993).

7. J. P. Mathias, E. E. Simanek, and G. M. Whitesides, *J. Amer. Chem. Soc.*, **116**, 4326 (1994).

8. U. Kumar, T. Kato, and J. M. J. Frechet, *J. Amer. Chem. Soc.*, **114**, 6630 (1992).

9. T. Kato and J. M. J. Frechet, *J. Amer. Chem. Soc.*, **111**, 8533 (1989).

10. S. C. Zimmerman, F. Zeng, D. E. C. Reichert, S. V. Kolotuchin, *Science*, **271**, 1095 (1996).

11. M. Szwarc, *Carbanion, Living Polymers, and Electron Transfer Processes*, Wiley-Interscience, New York (1968).

12. 90% by volume benzene and 10% by volume tetrahydrofuran (THF) were used as the polymerization solvents. THF was added to break up the aggregates that n-butyllithium forms in benzene (M. Morton, *Anionic Polymerization: Principles and Practice*, Academic Press, New York (1983)), thus increasing the rate of styrene oligomerization. The reaction was carried out at room temperature using standard Schlenk line techniques with a freeze-pump-thaw procedure of solvents prior to initiation.

13. R. P. Quirk and W. C. Chen, *Makromol. Chem.*, **22**, 85 (1989); P. J. Manson, *Polym. Sci., Poly. Chem. Ed.*, **18**, 1945 (1980).

14. The esterifications in scheme 1 are carried out under mild conditions developed by Moore and Stupp (*Macromolecules*, 23, 65 (1990)). The reaction utilizes

diisopropyl carbodiimide (DIPC), and 4-(N,N dimethylamino)pyridinium-4-toluenesulfonic acid (DPTS).

15. The diblock sequences in figure 4 represent a sampling from a population generated assigning probabilities to the various degrees of polymerization based on mass spectroscopy data. The tacticities of styrene sequences were simply assigned by a random number generator, and isoprene addition modes were assigned probabilities based on NMR data.

16. Field Desorption Ionization

17. Before crosslinking, triblock molecules **1** form a birefringent solid at room temperature which melts into a liquid crystal at 130°C and undergoes isotropization at 262°C.

18. The image processing technique known as fast Fourier transform enhances the signal to noise ratio in transmission electron microscopy images by removing the coefficients of the Fourier transform at those spatial frequencies that do not correspond to the periodic structure of a specimen (D. L. Misell in *Practical Methods in Electron Microscopy*, A. M. Glauert, Ed., North-Holland, New York (1978) vol. 7; A. Rosenfeld and A. C. Kak, *Digital Picture Processing*, Academic Press, New York (1982) 2nd ed, vol. 1; J. C. Russ, *The Image Processing Handbook*, CRC Press (1995) 2nd Ed.). Coefficients of the transform corresponding to structural detail are filtered from those corresponding to noise by multiplying the power spectrum by a "mask" having a value of unity near the coefficients of interest and zero elsewhere (the power spectrum is obtained from the fast Fourier transform of the digitized image and is analogous to an optical diffraction pattern).

19. Further details on these calculations are given in the last section of the manuscript.

20. L. H. Radzilowski, B. O. Carragher, and S. I. Stupp, *Macromolecules*, in press.

21. J. F. Elman, B. D. Johs, T. E. Long, and J. T. Koberstein, *Macromolecules*, **27**, 5341 (1994).

22. Samples were mounted onto a rotation/translation stage and the 1064nm fundamental was tightly focused onto the center of the sample yielding a peak intensity of 30MW/cm^2. The 1064nm fundamental was produced by a Molectron MY34-20 Q-switched Nd:YAG laser with a 20nsec pulse width operating at a 20Hz repetition rate. The second harmonic at 532nm was separated from the fundamental via a series of green pass filters and an Instruments SA, Inc. DH-10 double monochromator. The light was collected in a Hamamatsu R1477 photomultiplier tube and the signal was sent out to a digital data acquisition system and an oscilloscope. All data were corrected for transmission of fundamental and absorption of the second harmonic.

23. K. Kumagi, G. Mizutani, H. Tsukioka, T. Yamauchi, and S. Ushioda, *Phys. Rev. B*, **48** (9), 14488 (1993).

24. D. Wilk, D. Johannsmann, C. Stanners, and Y. R. Shen, *Phys. Rev. B*, **51** (15), 10057 (1995).

25. H. Hoshi, T. Yamada, K. Ishikawa, H. Takeoze, and A. Fukuda, *Phys. Rev. B*, **52** (16), 12335 (1995).

26. H. Hoshi, T. Yamada, K. Ishikawa, H. Takezoe, and A. Fukuda, *Phys. Rev. B*, **53** (9), 12663 (1996).

27. M. Keser and S. I. Stupp, unpublished results.

28. SIMPLEX minimization is first used for a few steps and this often requires fixing awkward structures such as back folded CH_2 units, hydrogen pierced rings, and fused rings.

29. The presence of chloroform in cast films was established by infrared bands at 758 cm^{-1}, 1215 cm^{-1}, and 3025 cm^{-1}.

30. S. Wu, *Polymer Interface and Adhesion*, Marcel Dekker, New York (1985).

31. G. C. Pimentel and A. L. McClellan, *The Hydrogen Bond*, W. H. Freeman, San Francisco (1960).

32. Supported by grants from the Office of Naval Research (N00014-96-1-0515), the National Science Foundation (DMR 89-20538), and the Department of Energy (DEFG02-91ER45439) obtained through the Materials Research Laboratory of the University of Illinois. FDI experiments were carried out by Kyle Gresham of our laboratory.

Figure Captions

Figure 1. Molecular graphics rendition of nanostructures having various shapes which may be supramolecular or covalent entities. Most of the nanostructures formed have been experimentally observed.

Figure 2. Molecular nanostructures with well defined shapes and sizes are likely to pack into predictable structures. Plates are likely to stack with a common stacking direction, and tube or rod-like nanostructures would tend to uniaxially align. Regularly sized and shaped nanostructures may organize into superlattices of varying geometries and symmetries.

Figure 3. Molecular graphics rendition of the triblock self assembling molecule, containing an aromatic rod-like segment, covalently attached to short sequences of isoprene and styrene, both containing great structural diversity and differing in cross section relative to rod segments.

Figure 4. A sampling of 20 chemical sequences that could exist in the triblock molecular system. These sequences were generated using a Poisson distribution of molar mass for the styrene and isoprene segments, assuming a random sequence of meso and racemic diads for oligostyrene's tacticity and a random mixture of 1,4 and 3,4 isoprene addition products (with a trace of 1,2) for the second block coil block. At the rod junction the rigid segment is identical in all molecules of the system.

Figure 5. a) Transmission electron micrograph at low magnification (with a high magnification inset) of films formed by the triblock molecules, revealing regularly sized and shaped aggregates that self organize into monoclinic superlattice domains. b) Similar micrograph obtained at intermedite magnification relative to those in a) (all micrographs were taken from the thinnest portions of the films).

Figure 6. Wide angle electron diffraction pattern obtained from the aggregates shown in the images of figure 5, indicating the aggregates contain crystalline regions.

Figure 7. Small angle electron diffraction pattern of the aggregates shown in the images of figure 5, revealing their self organization into a monoclinic superlattice with parameters equal to 70 and 66 Å, and a characteristic angle of 110°.

Figure 8. Wide angle diffraction pattern of the aggregates following annealing at 250°C for a period of 2 hours.

Figure 9. Transmission electron micrograph of an ultramicrotomed section obtained from a one micron thick film using a diamond knife (bottom).

A section of the image viewed under higher magnification (middle), and its Fourier filtered image obtained only with meridional intensity in the Fourier transform in order to highlight the lamellar periodicity of the film.

Figure 10. TEM image of an ultramicrotomed film formed by triblock molecules and its corresponding fast Fourier transforms (FFT) (top). Partially masked FFTs and their corresponding inverse FFTs (bottom).

Figue 11. Molecular model of the supramolecular unit composed of 100 triblock molecules and a molar mass of about 200 kilodaltons. Rod segment packing in the mushroom stem is based on electron diffraction data, and its rectangular shape on the observation of a monoclinic superlattice of the nanostructures.

Figure 12. Schematic representation of how mushroom nanostructures formed by triblock molecules might organize to form the macroscopic film. The nanostructures are stacked with polar order always producing a surface of caps and an opposite surface of stems. The three dimensional details of nanostructure stacking are not known but within one layer we have observed a monoclinic arrangement of the aggregates.

Figure 13. Water droplets and their contact angles when placed on opposite surfaces of a film cast on a hydrophilic surface. The surface on the left is hydrophobic and corresponds to the air side of the film, the one on the right is the hydrophilic surface exposed when the film is inverted.

Figure 14. Plot of time elapsed before films of poly(vinyl phenol) detach from glass after being immersed in aqueous HF of varying molarities (red line). Annealed supramolecular films never detach from glass, and the plot in blue indicates instead the times elapsed before the glass fractures upon HF immersion.

Figure 15. Schematic representation of the second order nonlinear optical experiment carried out on annealed supramolecular films.

Figure 16. Intensity of the second harmonic beam as a function of surface position of the incident infrared laser beam on the film's surface.

Figure 17. Profilometer scan showing variations in thickness across the surface of the supramolecular film.

Figure 18. Intensity of the second harmonic generation signal from the unpoled film as a function of film thickness.

Figure 19 Schematic representation of chemically bipolar, cavitated, or protruded nanostructures arranged in polar stacks. If polar stacking occurs, surface roughness or single layer wear reexposes the same surface which may be an array of cavities, protrusions, or some specific chemical structure which differs from that on the opposite film surface.

Figure 20. Molecular graphics of a cluster of triblock molecules before complete energy minimization, color-coded for energy in different sectors of the cluster (left). A relaxed cluster revealing the mushroom architecture (right).

Figure 21. Schematic representation of the relative orientation of diblock coil or rod segments in the ferro and antiferro clusters shown in figure 22.

Figure 22. Two different molecular clusters composed of 13 coil-like diblock segments (right) arranged parallel to each other (ferro cluster), or antiparallel to each other (antiferro cluster). At left the same two types of clusters are shown for the rod segments of triblock molecules. The calculated energies associated with these four clusters and their cross sectional densities predict that the mushroom cluster of triblock molecules would be favored by the system.

Figure 23. Schematic representation depicting the smaller and more easily filled pores in monolayer stacking of nanostructures compared to pores formed in bilayer stacking. In bilayer stacking of these asymmetric nanostructures, displacements parallel or perpendicular to the layer normal are not efficient at filling volume otherwise occupied by solvent (orange regions).

Scheme 1

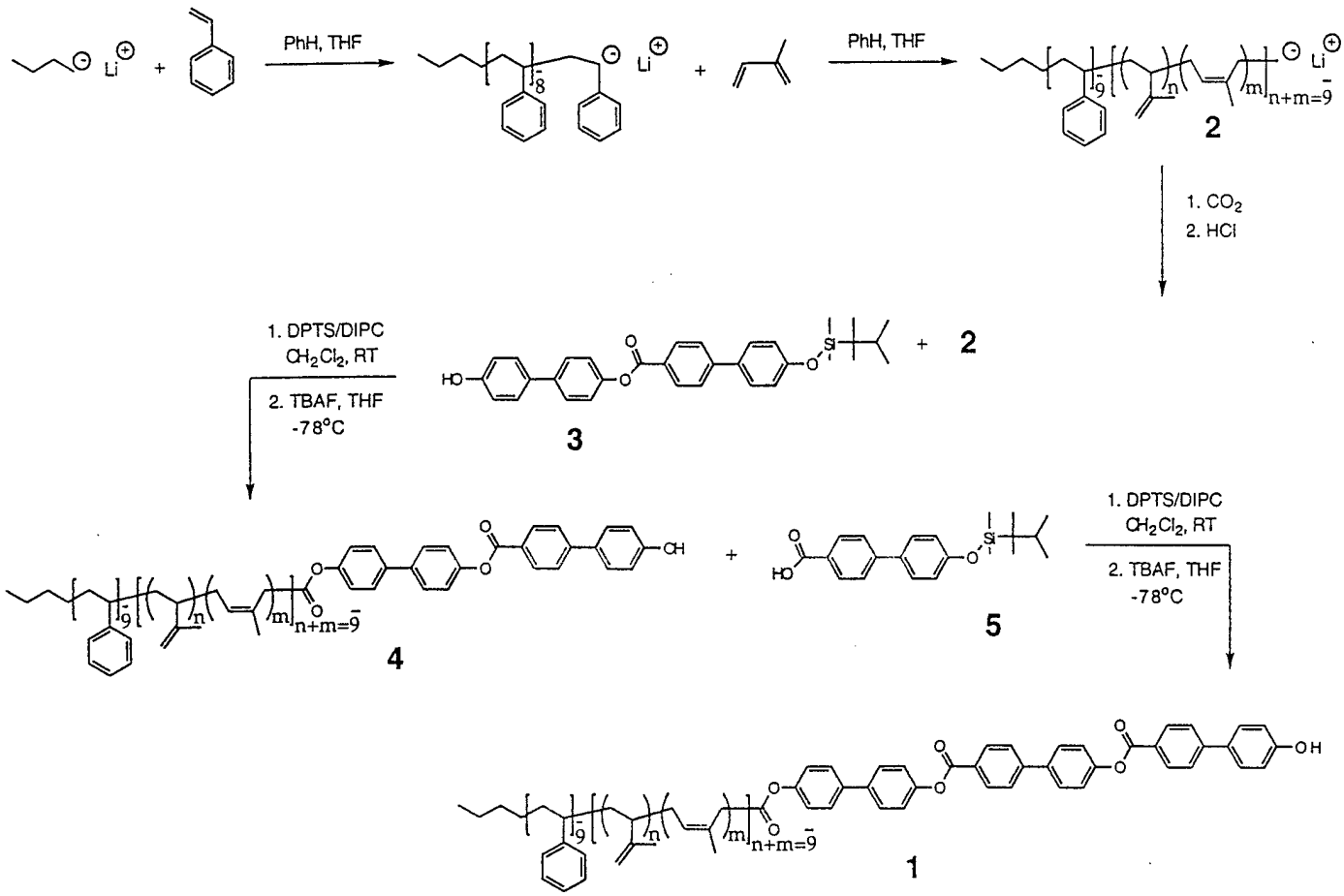
PhH, THF
PhH, THF
1. CO_2
2. HCl
1. DPTS/DIPC
CH_2Cl_2, RT
2. TBAF, THF
-78°C
1. DPTS/DIPC
CH_2Cl_2, RT
2. TBAF, THF
-78°C
2
3
4
5
1

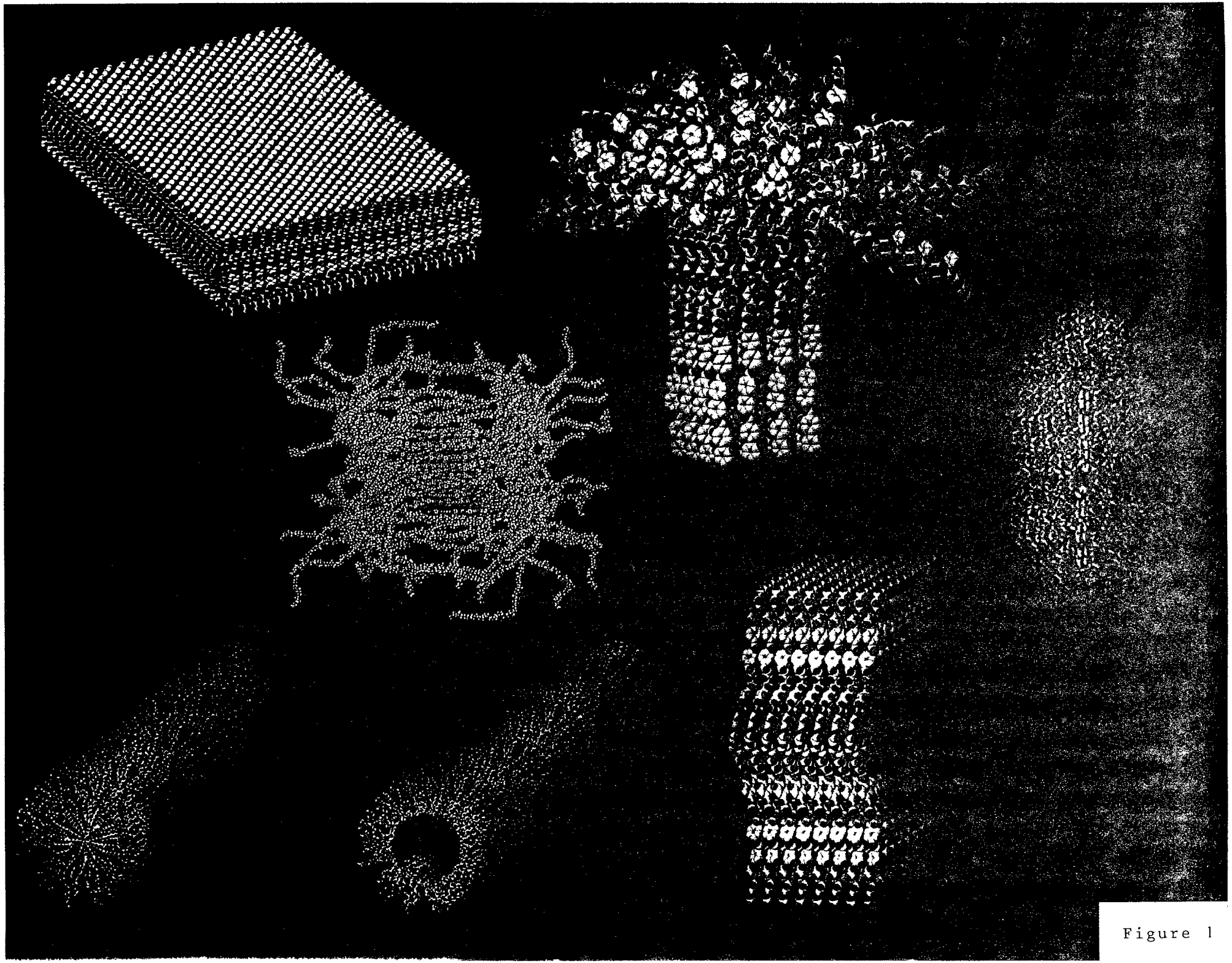

Figure 1

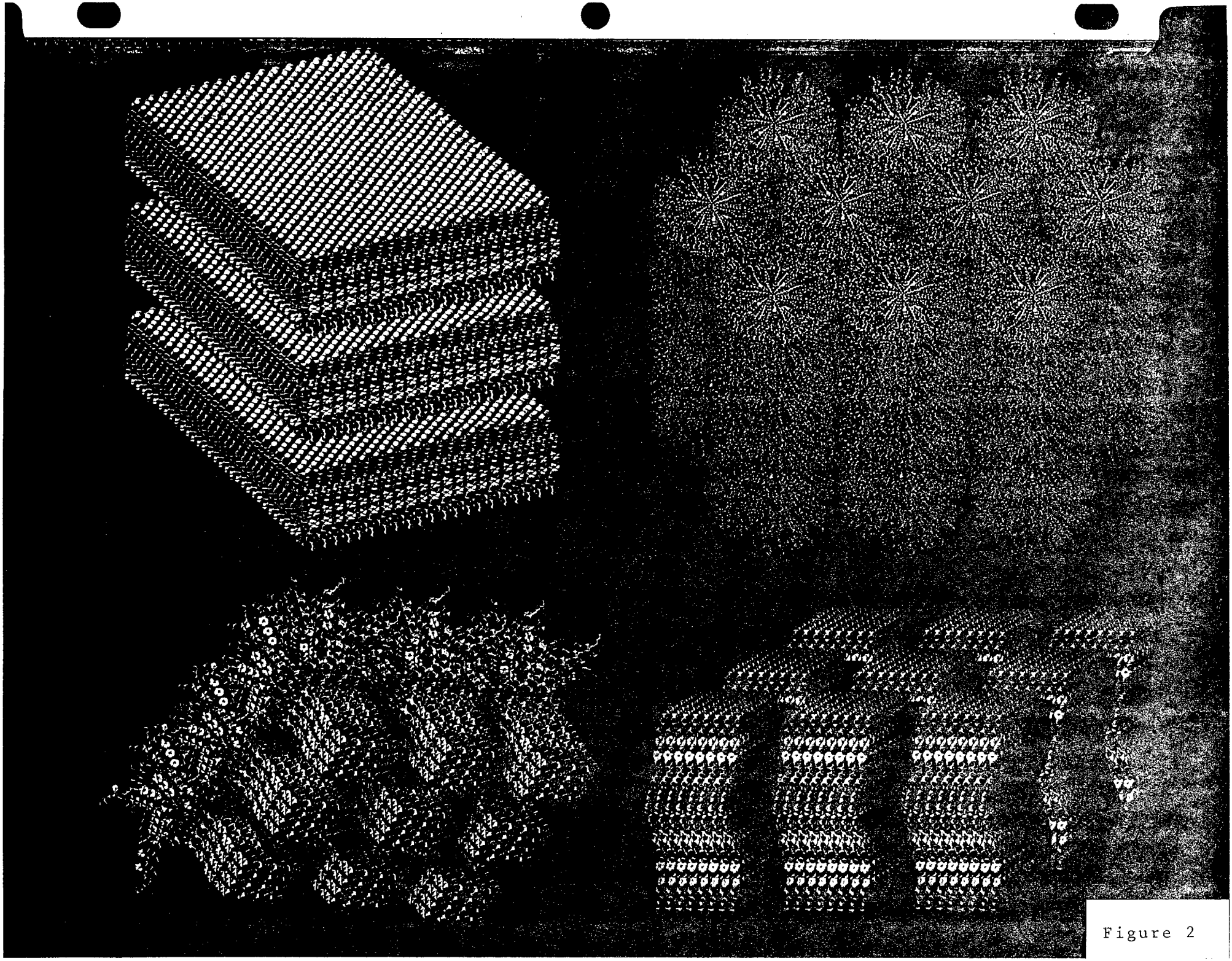

Figure 2

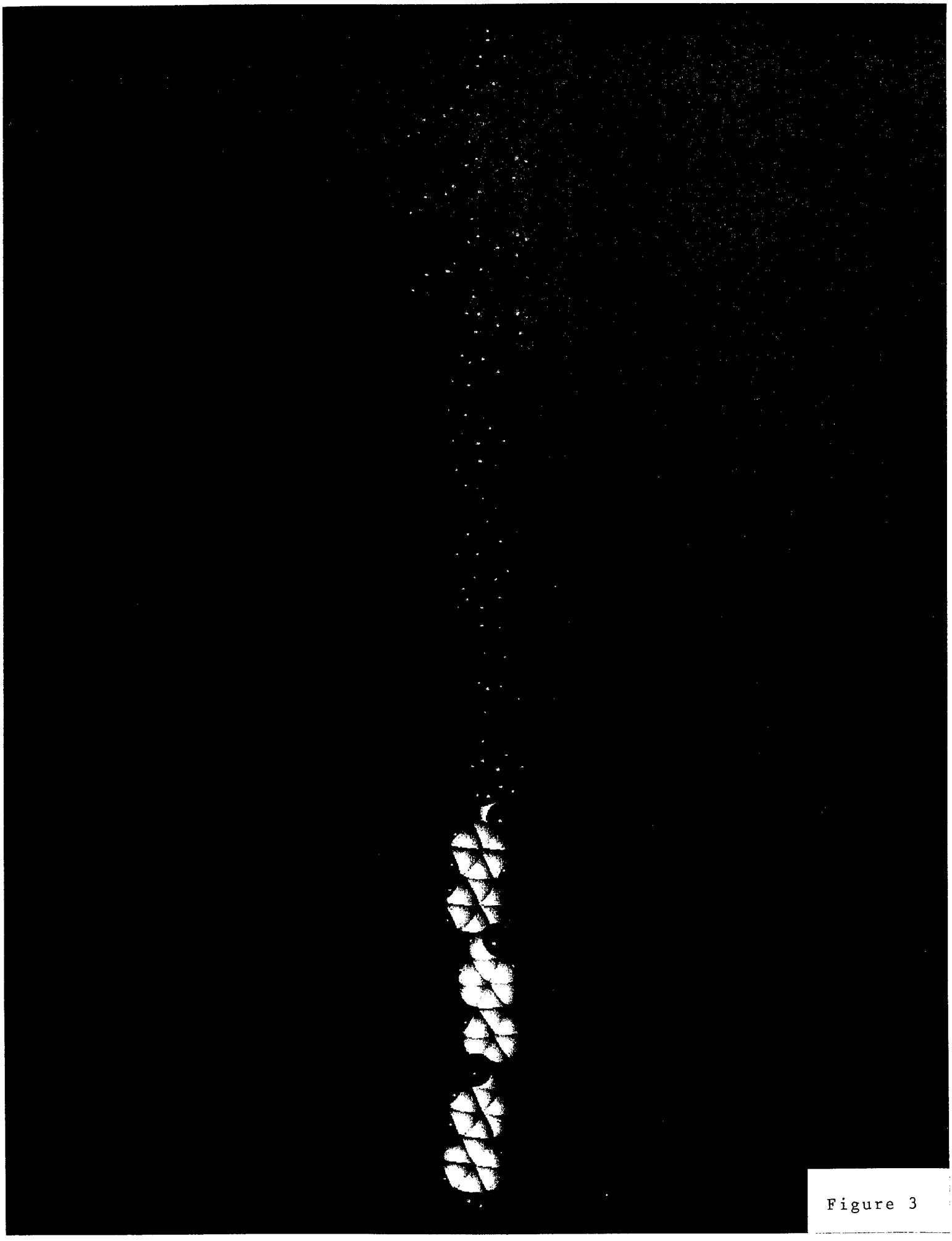

Figure 3

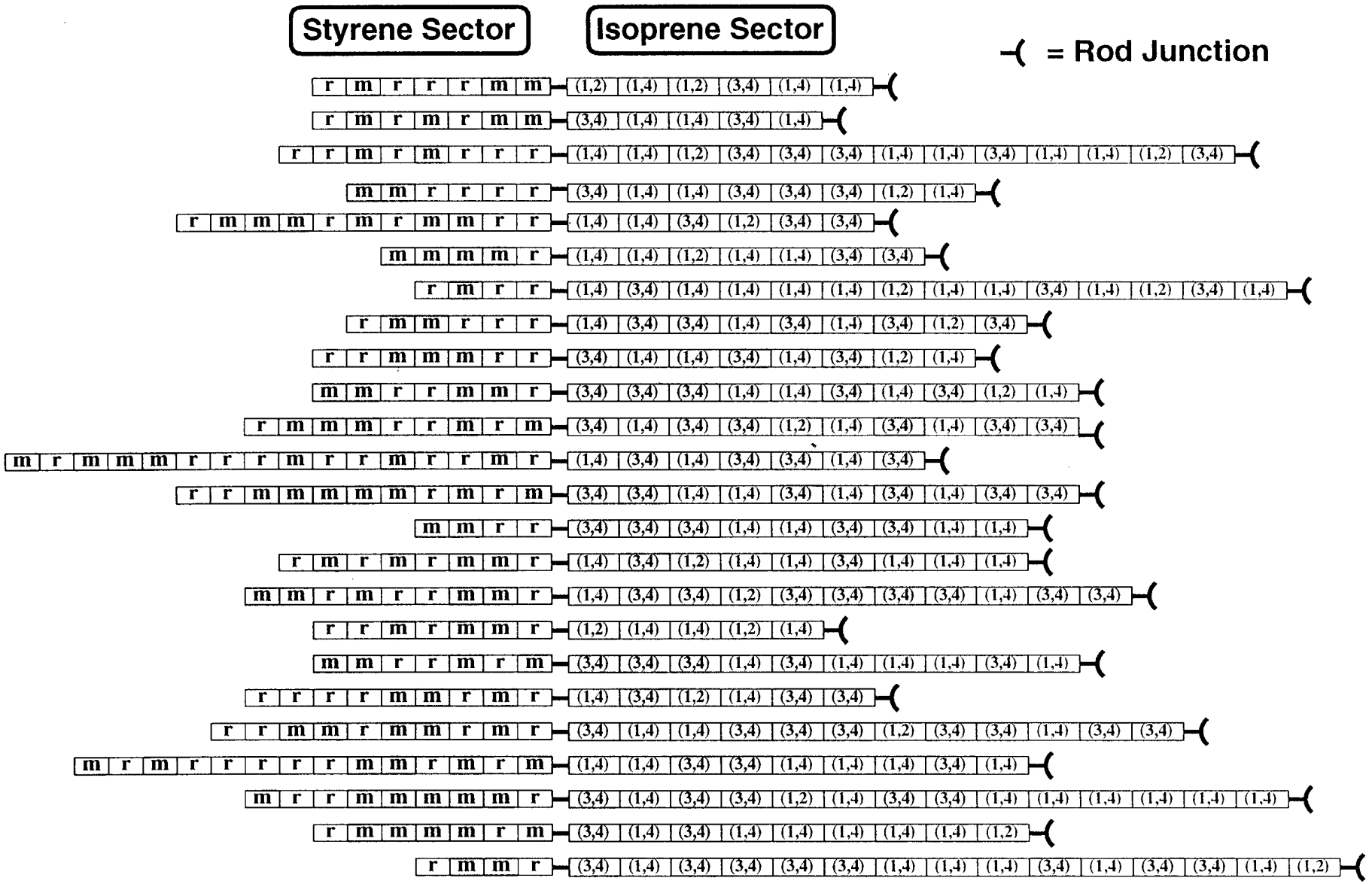

Figure 4

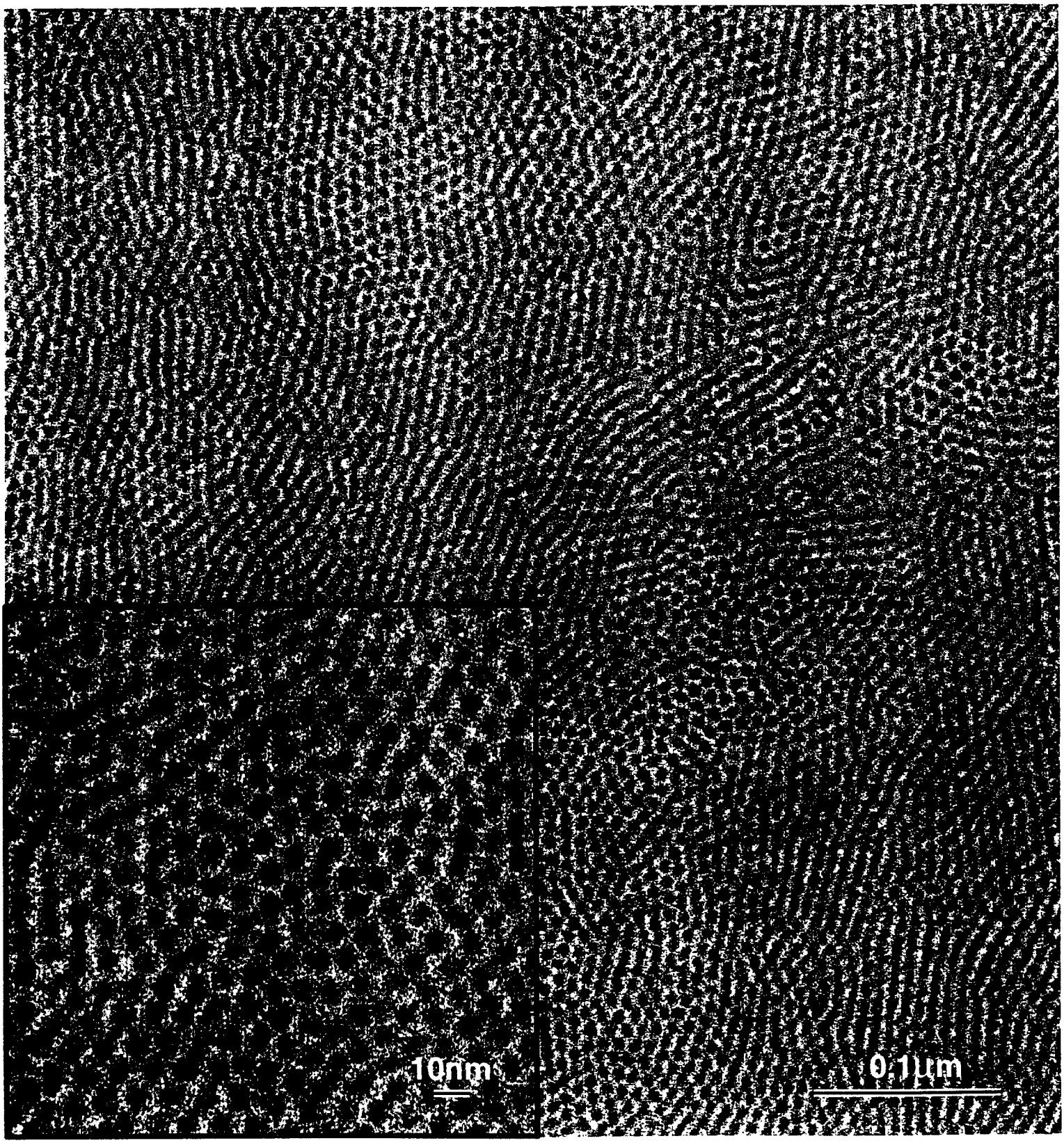

Figure 5a

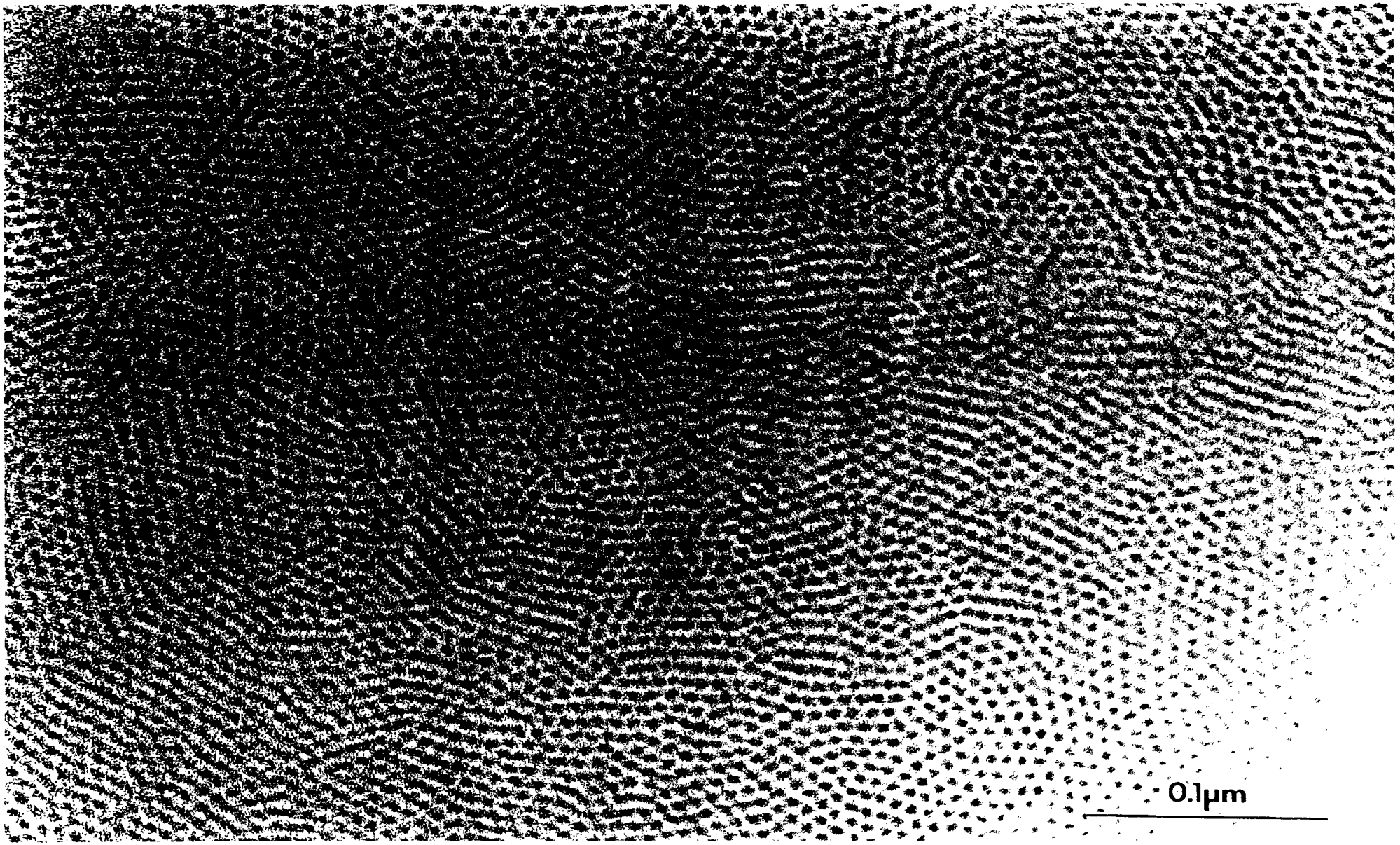

Figure 5b

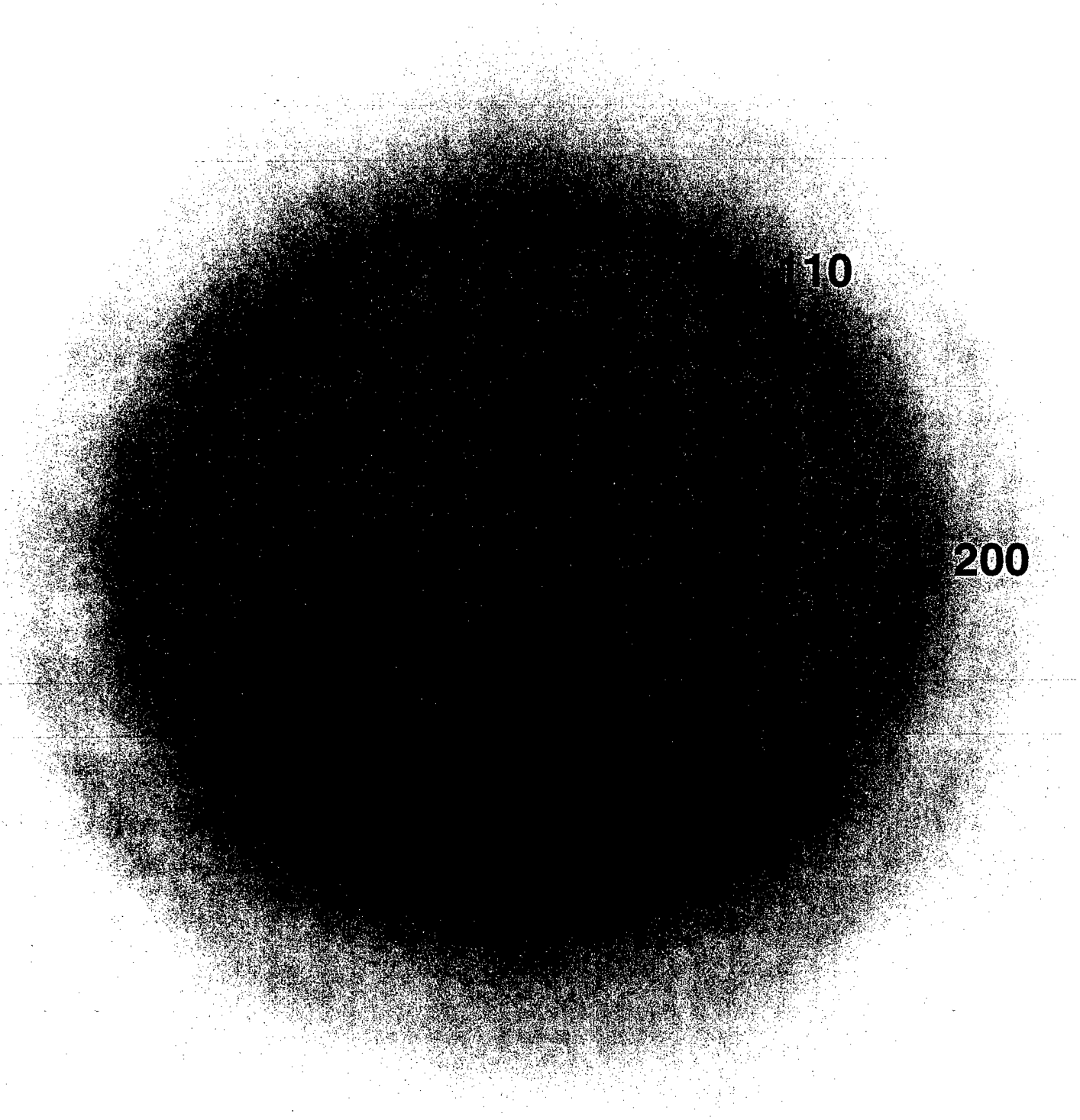

Figure 6

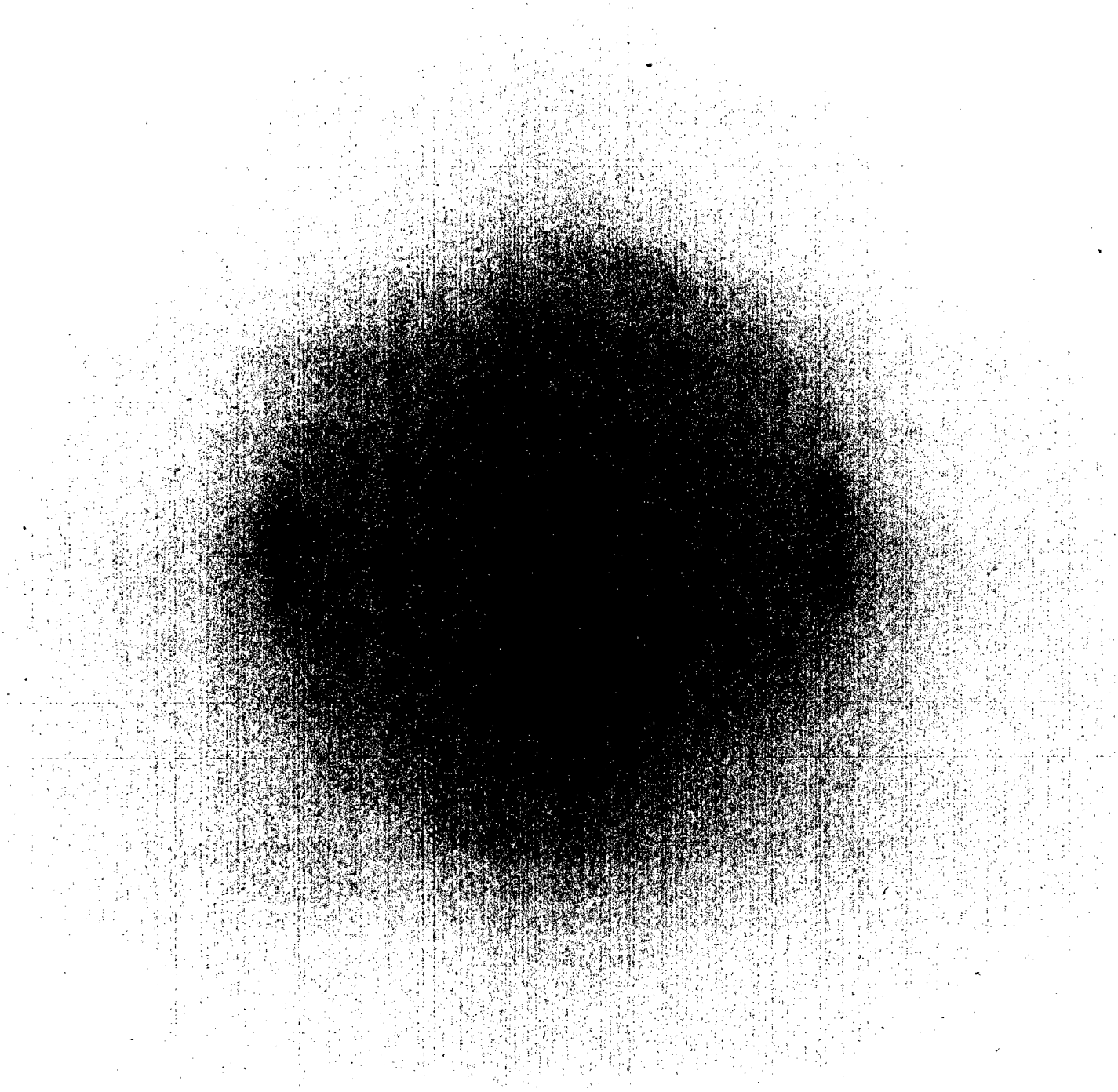

Figure 7

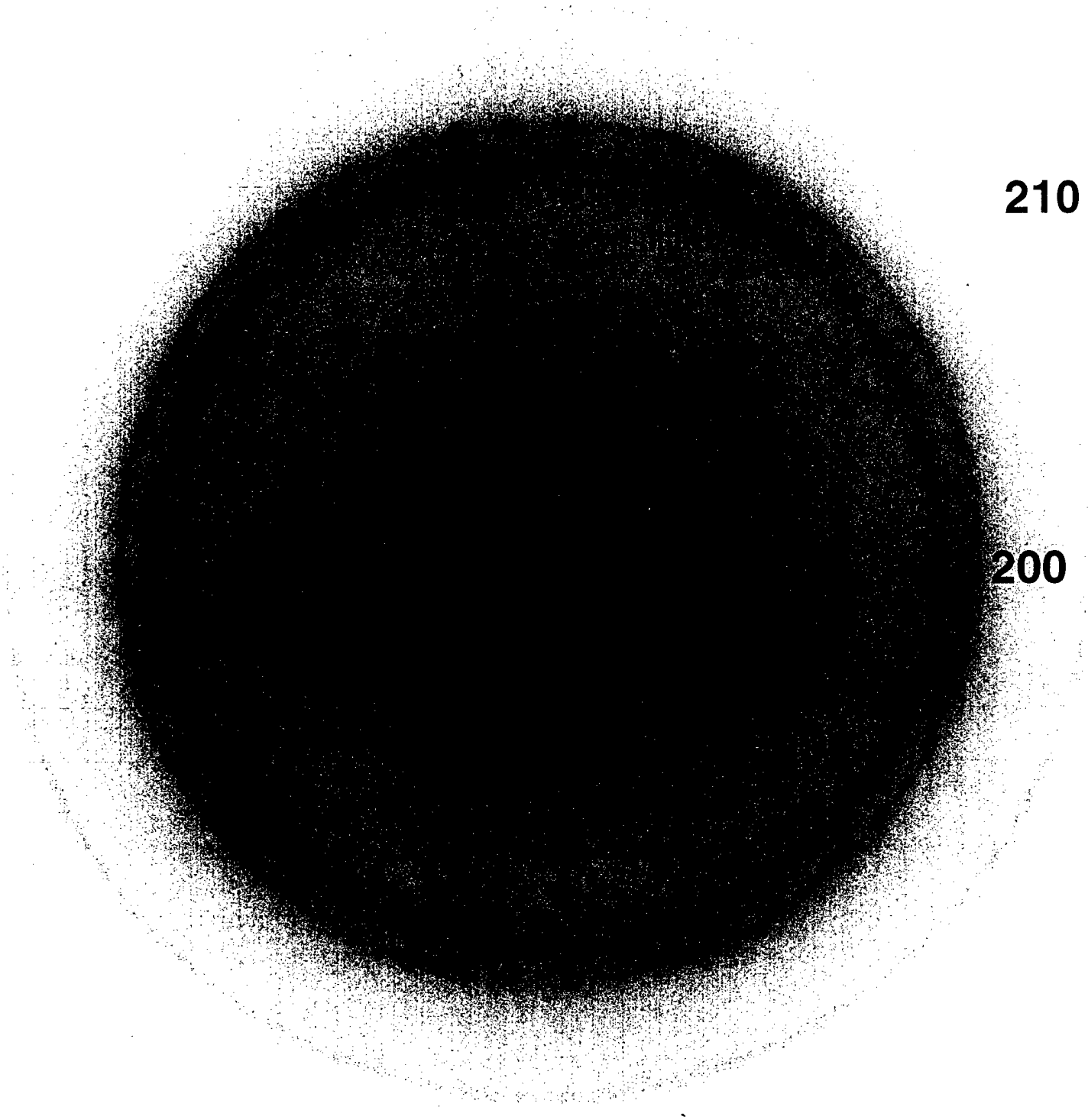

Figure 8

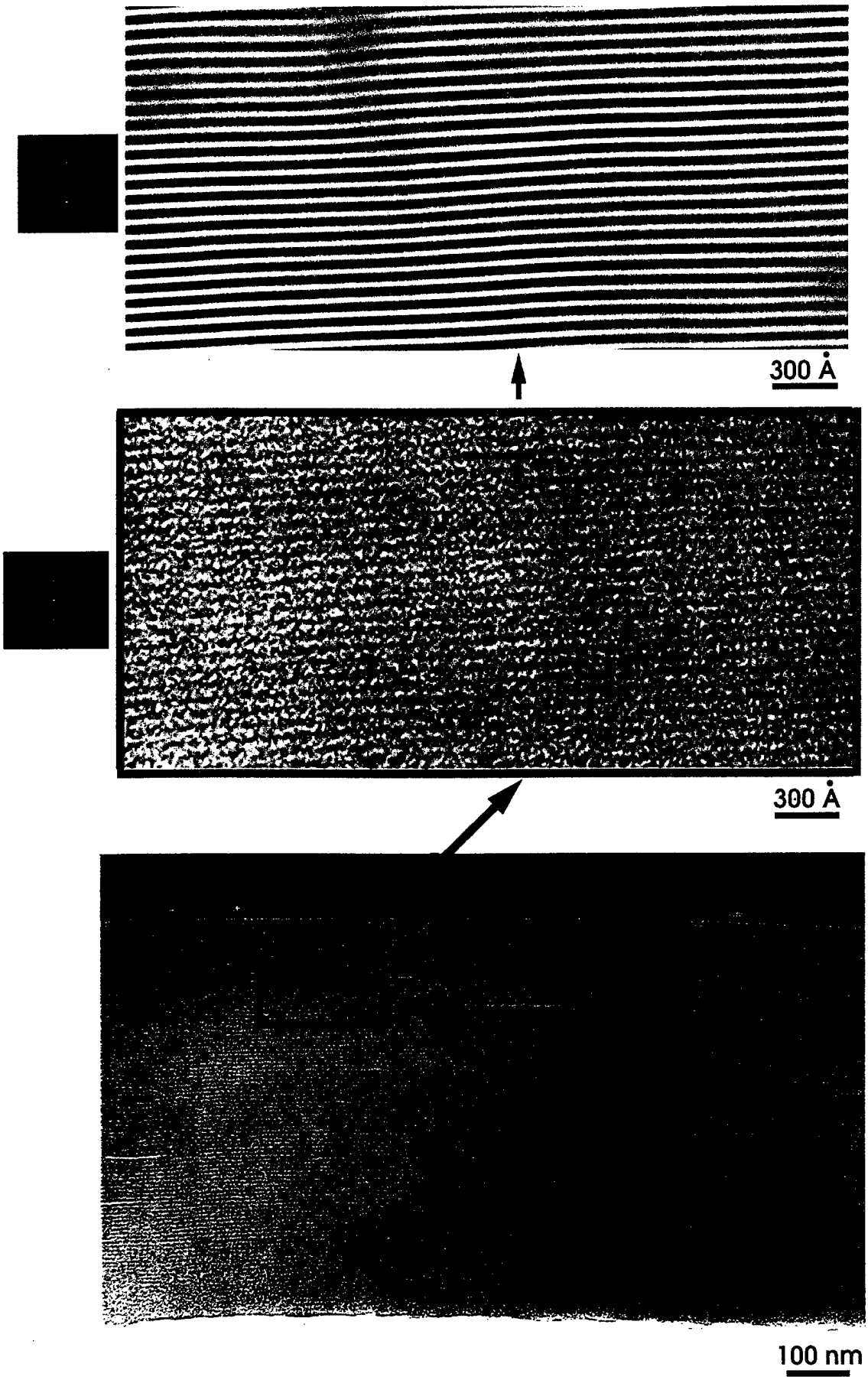

Figure 9

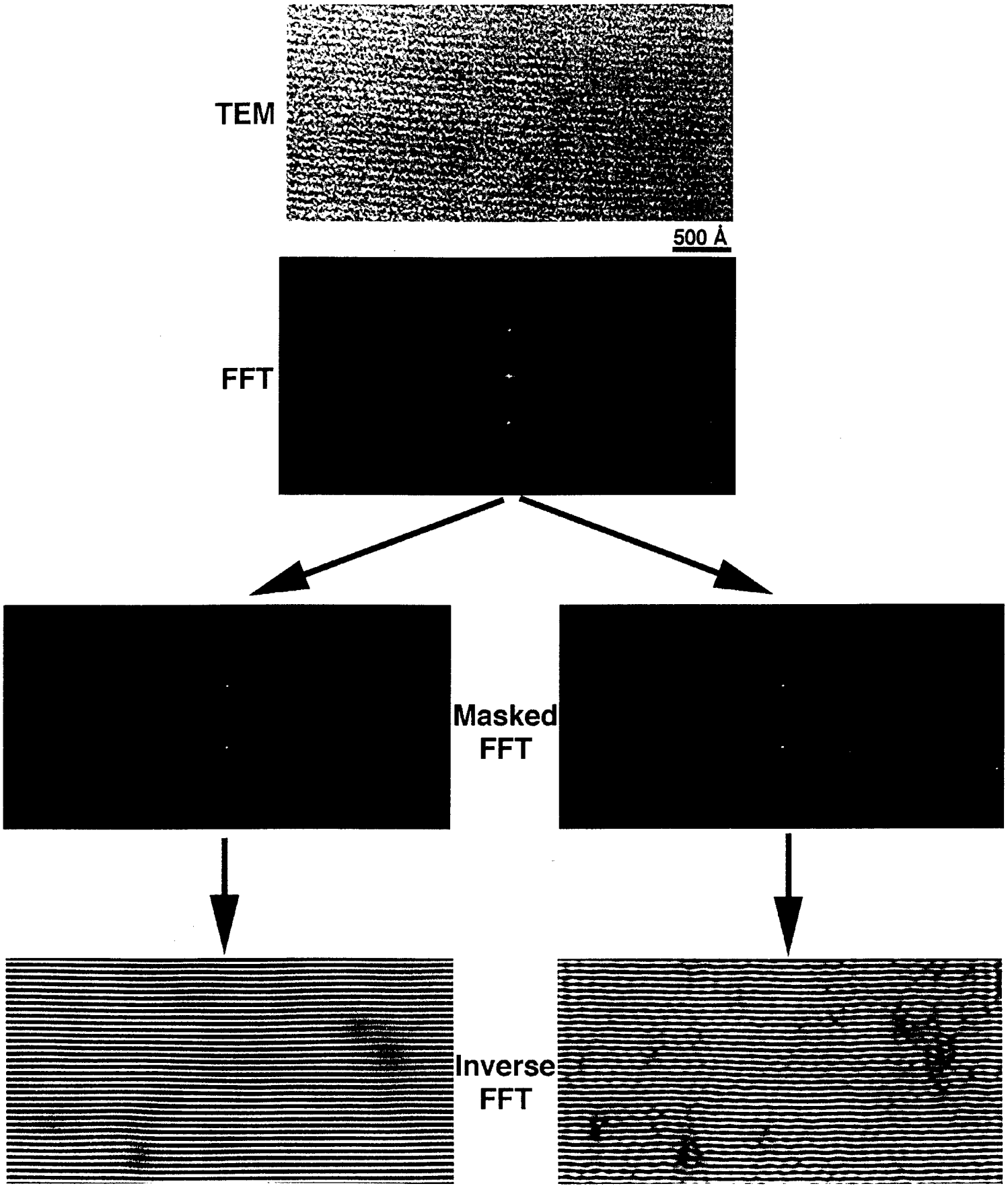

Figure 10

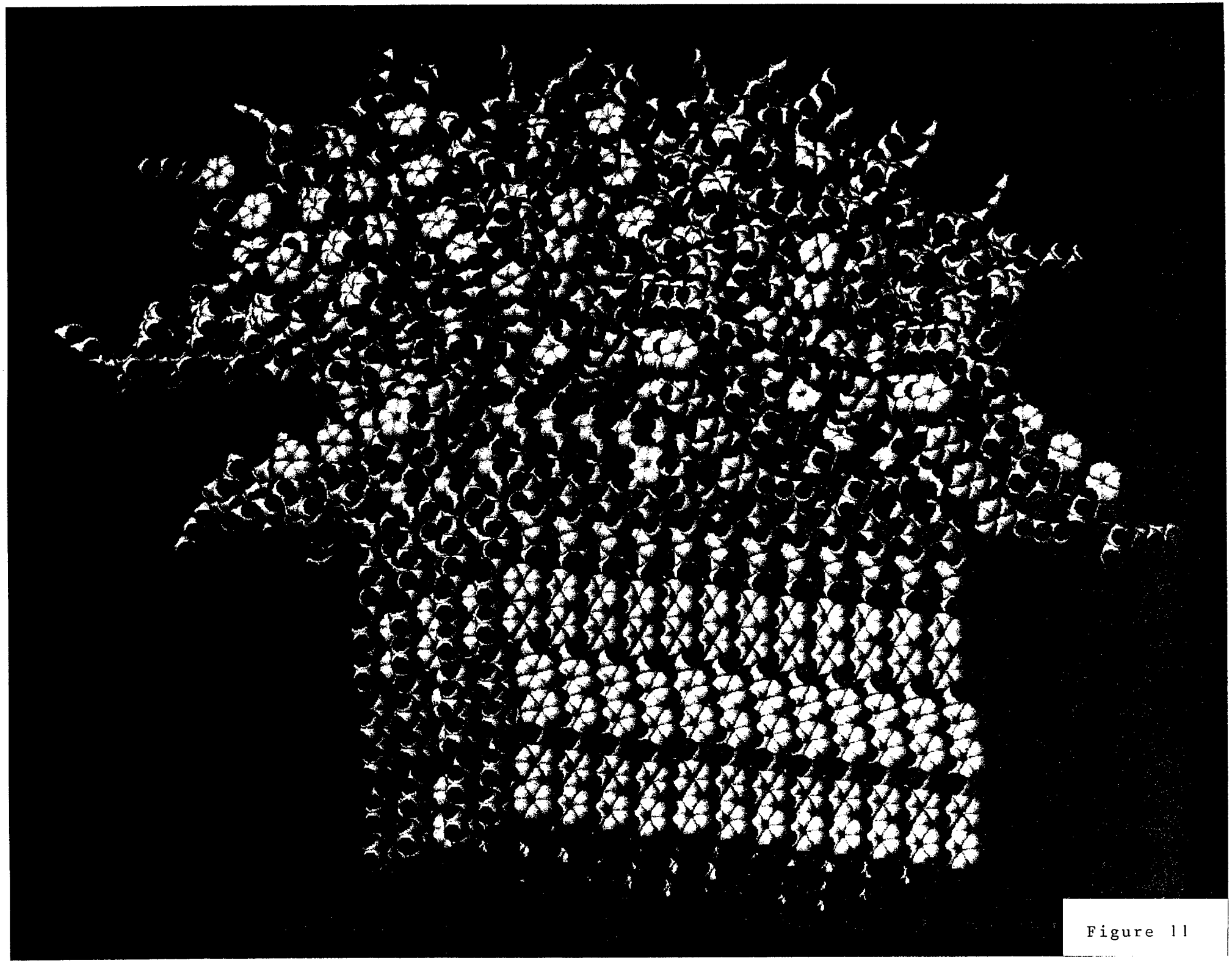

Figure 11

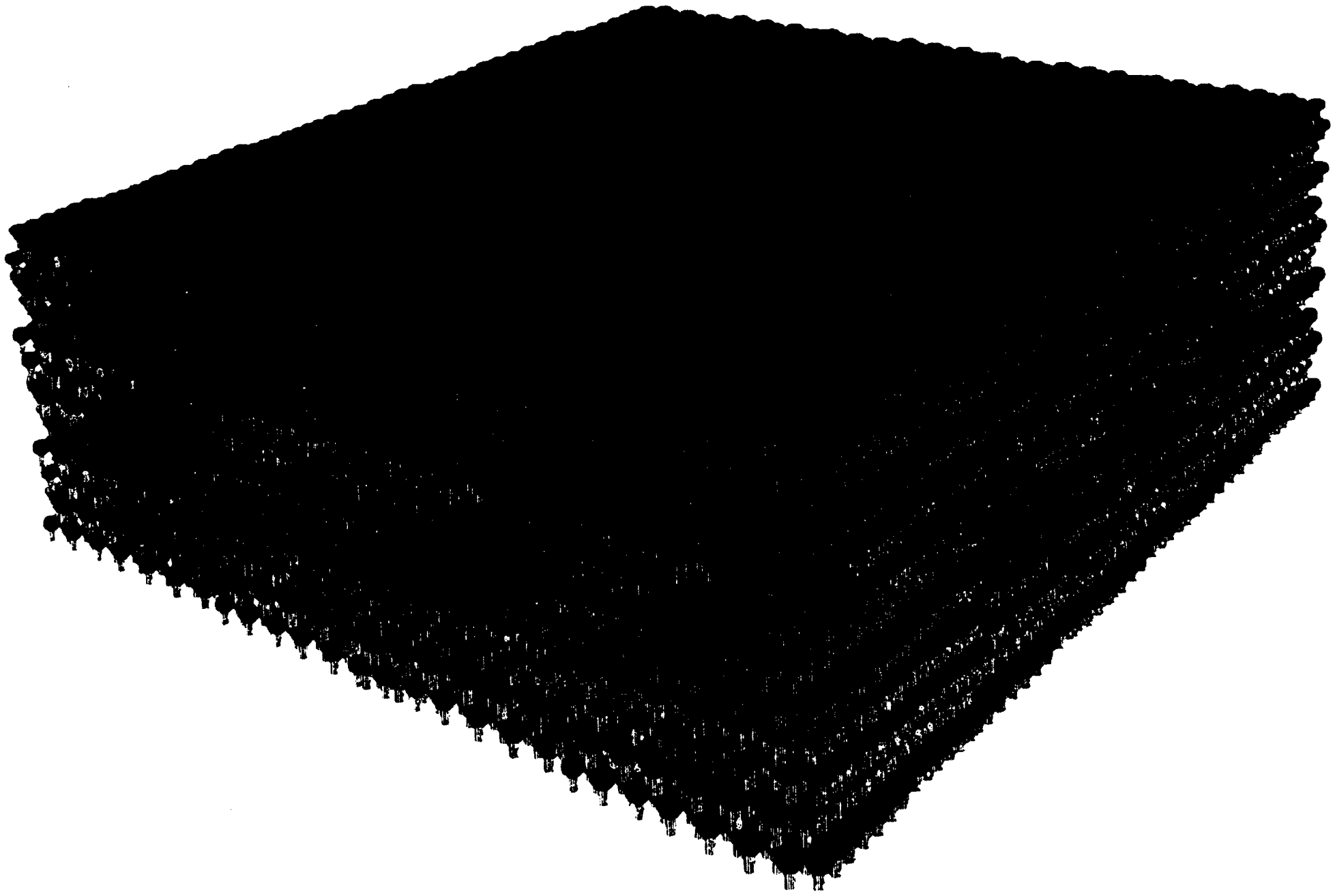

Figure 12

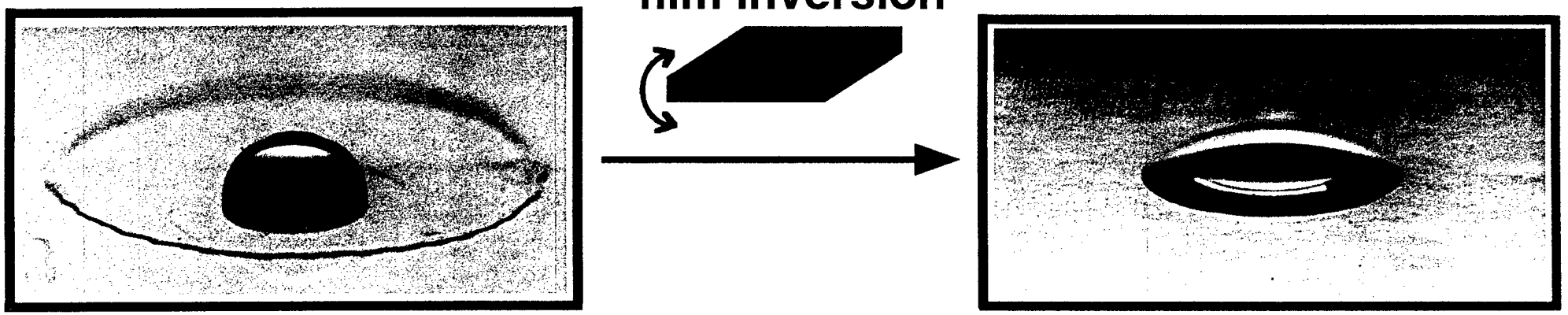

$\theta_{water} = 98° \pm 1°$

$\theta_{water} = 27° \pm 2°$

Figure 13

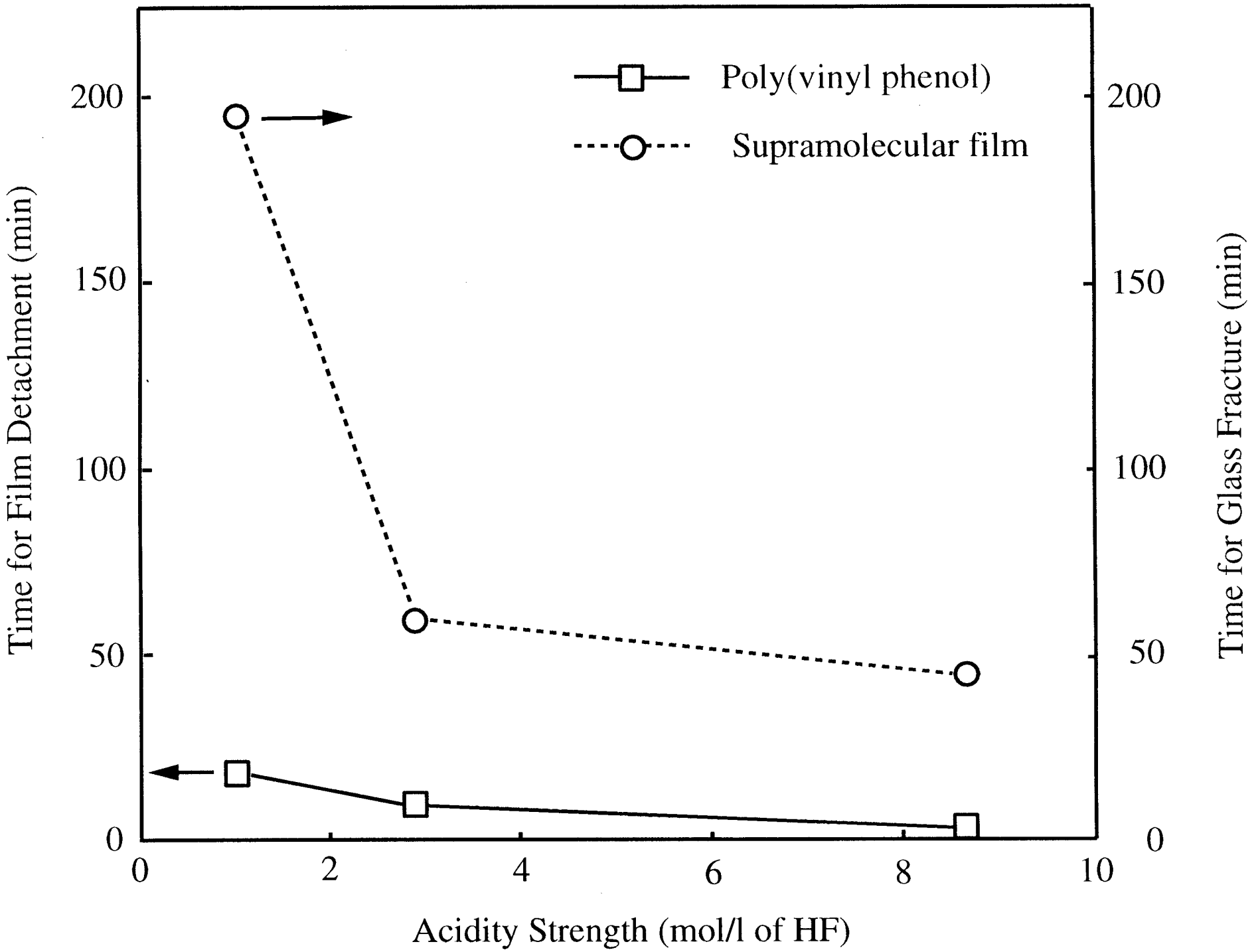
Poly(vinyl phenol)
Supramolecular film
Time for Film Detachment (min)
Time for Glass Fracture (min)
Acidity Strength (mol/l of HF)
0
50
100
150
200
0
2
4
6
8
10

Figure 14

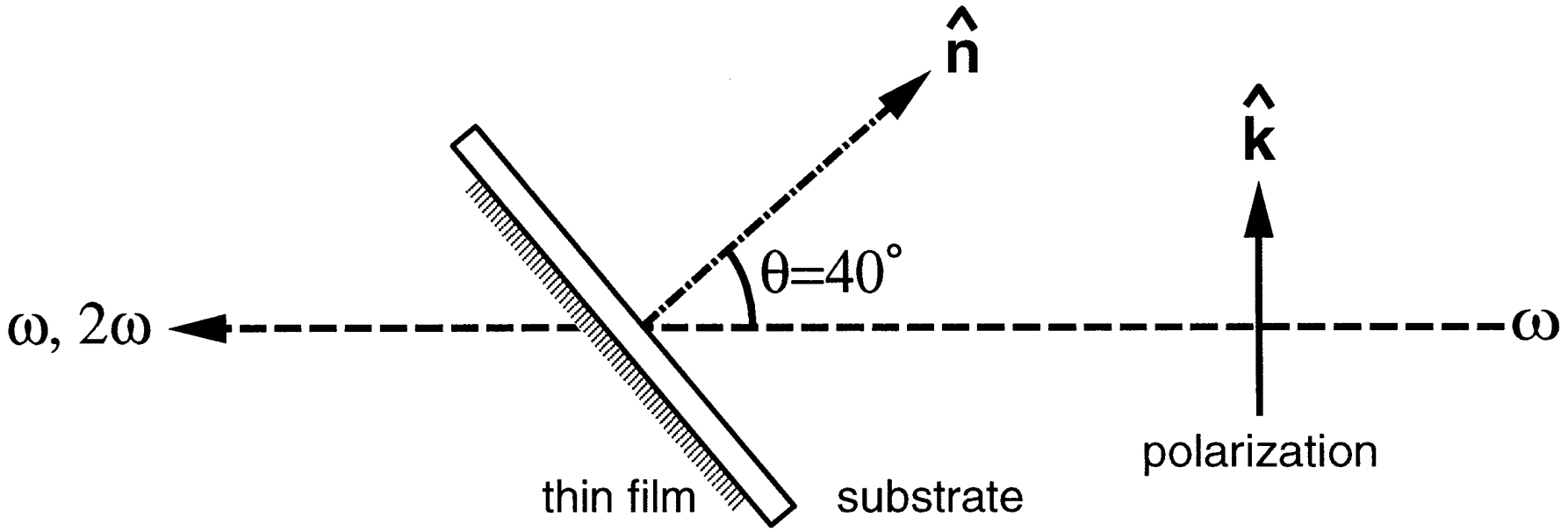

Figure 15

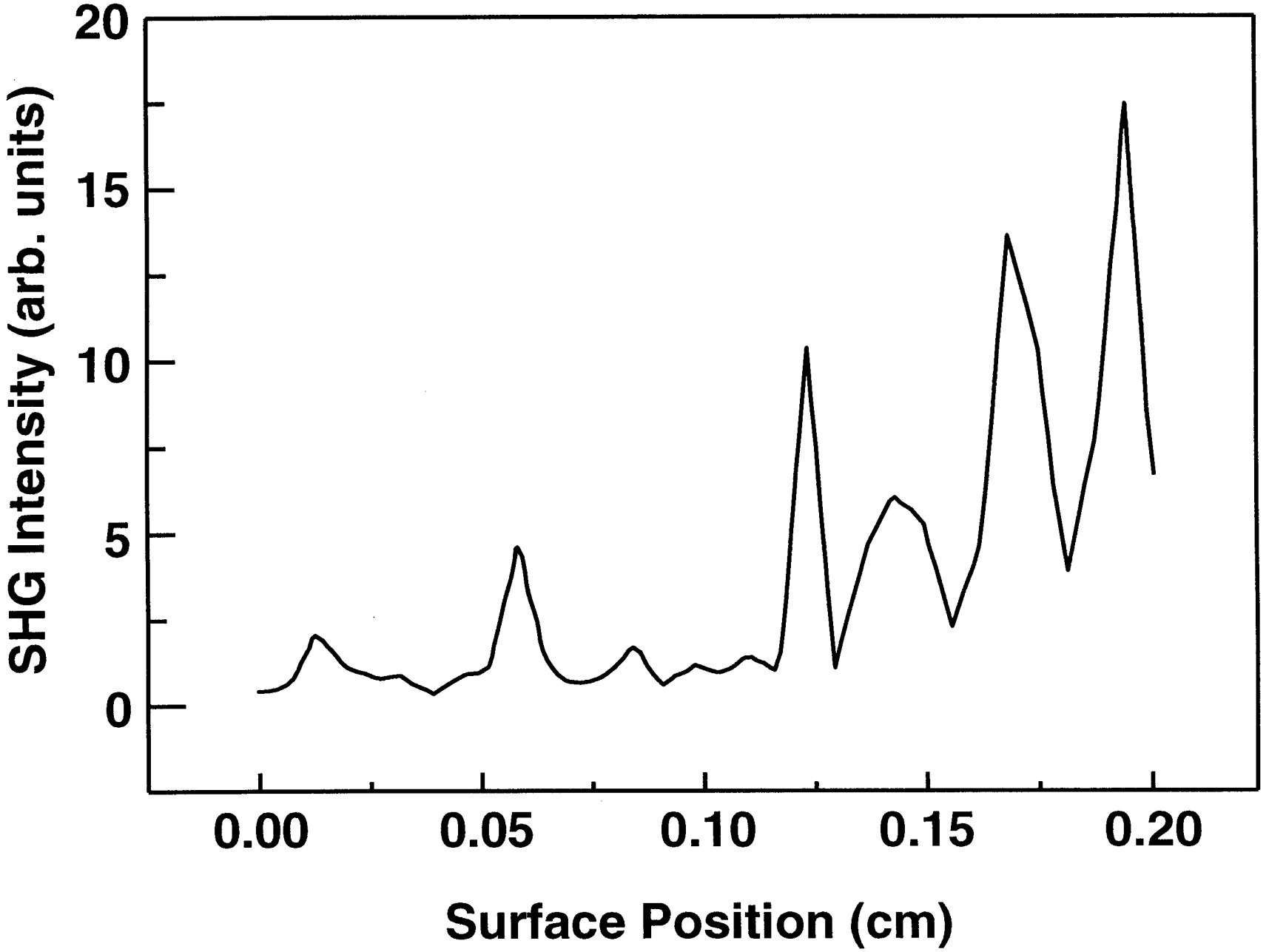
SHG Intensity (arb. units)
20
15
10
5
0
0.00
0.05
0.10
0.15
0.20
Surface Position (cm)

Figure 16

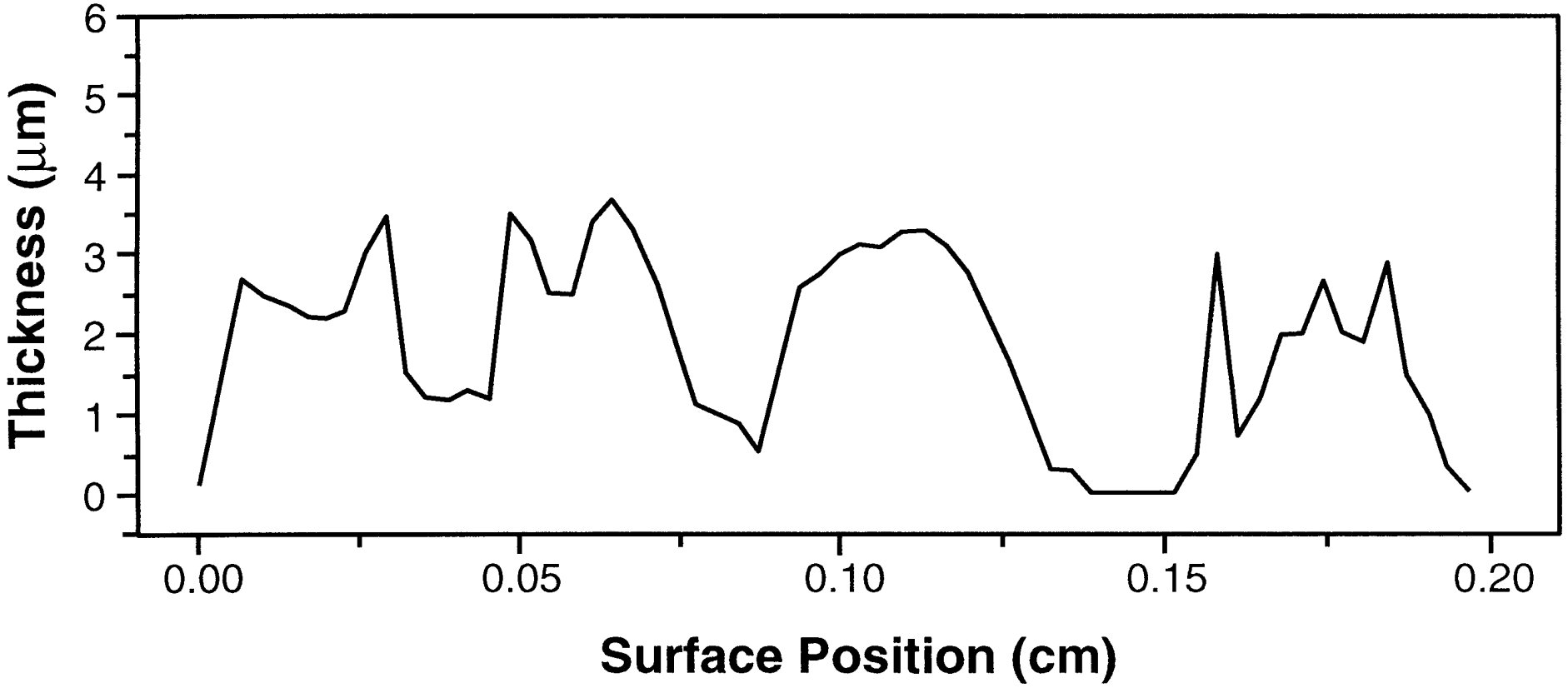
Thickness (μm)
6
5
4
3
2
1
0
0.00
0.05
0.10
0.15
0.20
Surface Position (cm)

Figure 17

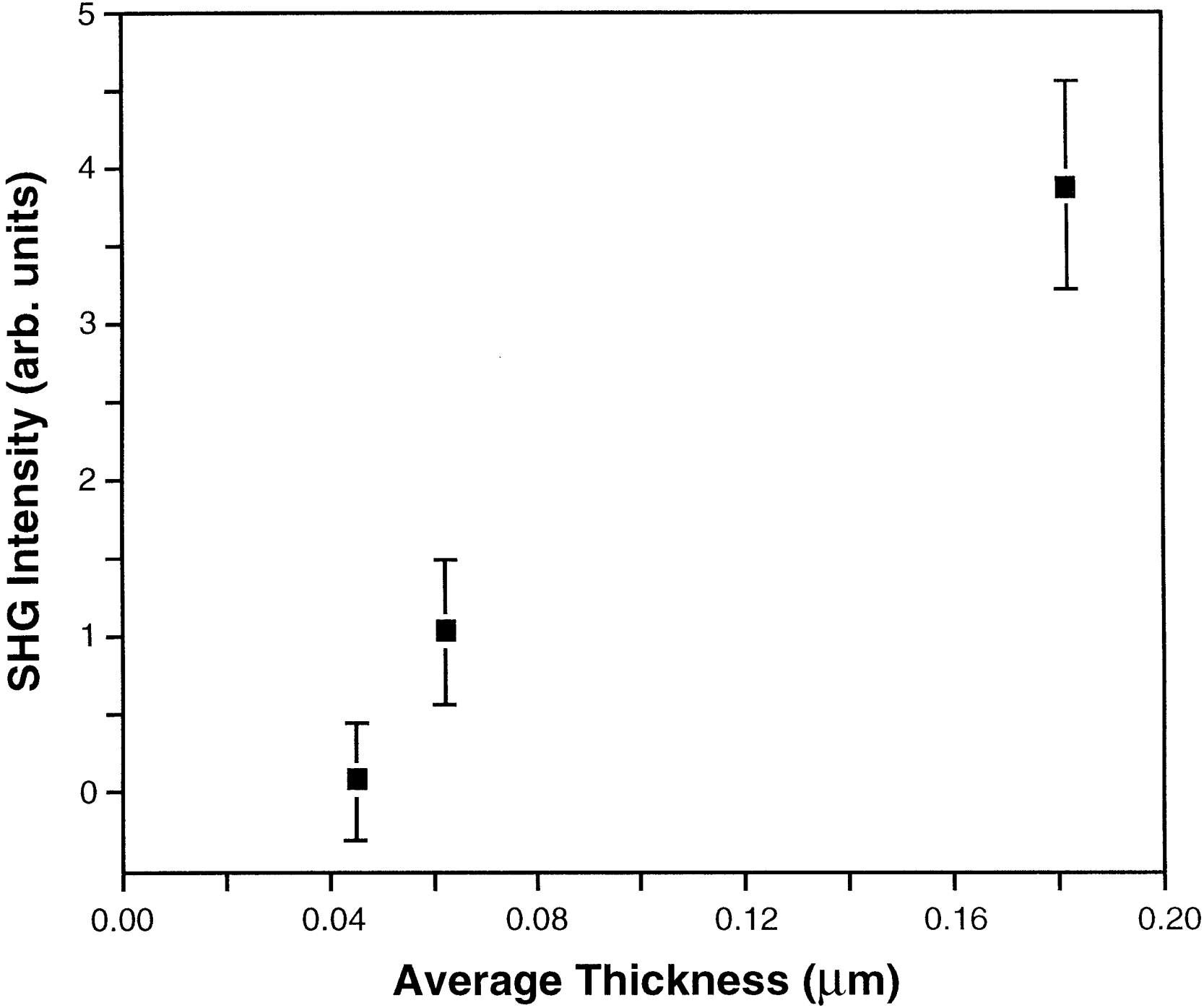
SHG Intensity (arb. units)
5
4
3
2
1
0
0.00
0.04
0.08
0.12
0.16
0.20
Average Thickness (μm)

Figure 18

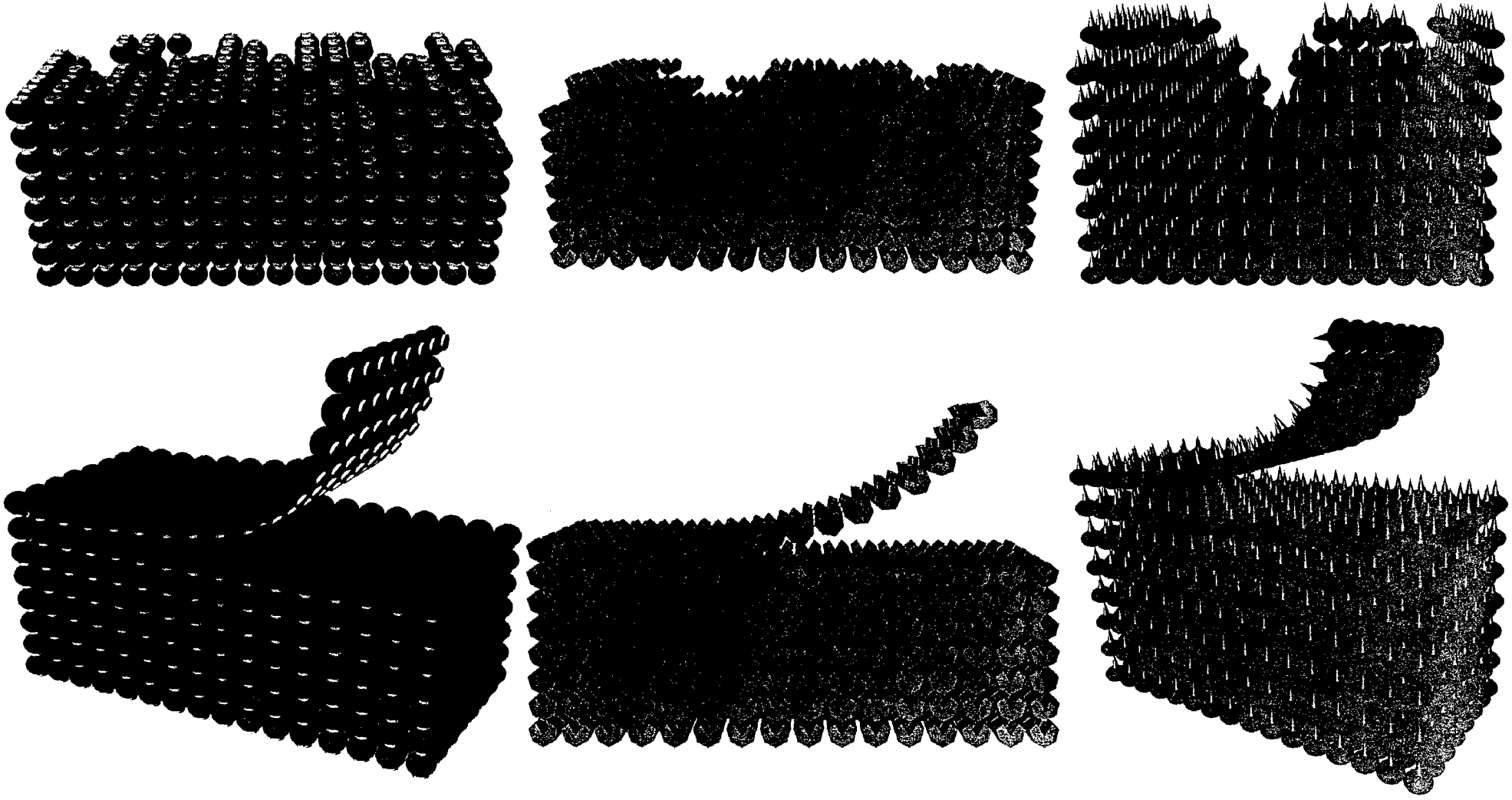

Figure 19

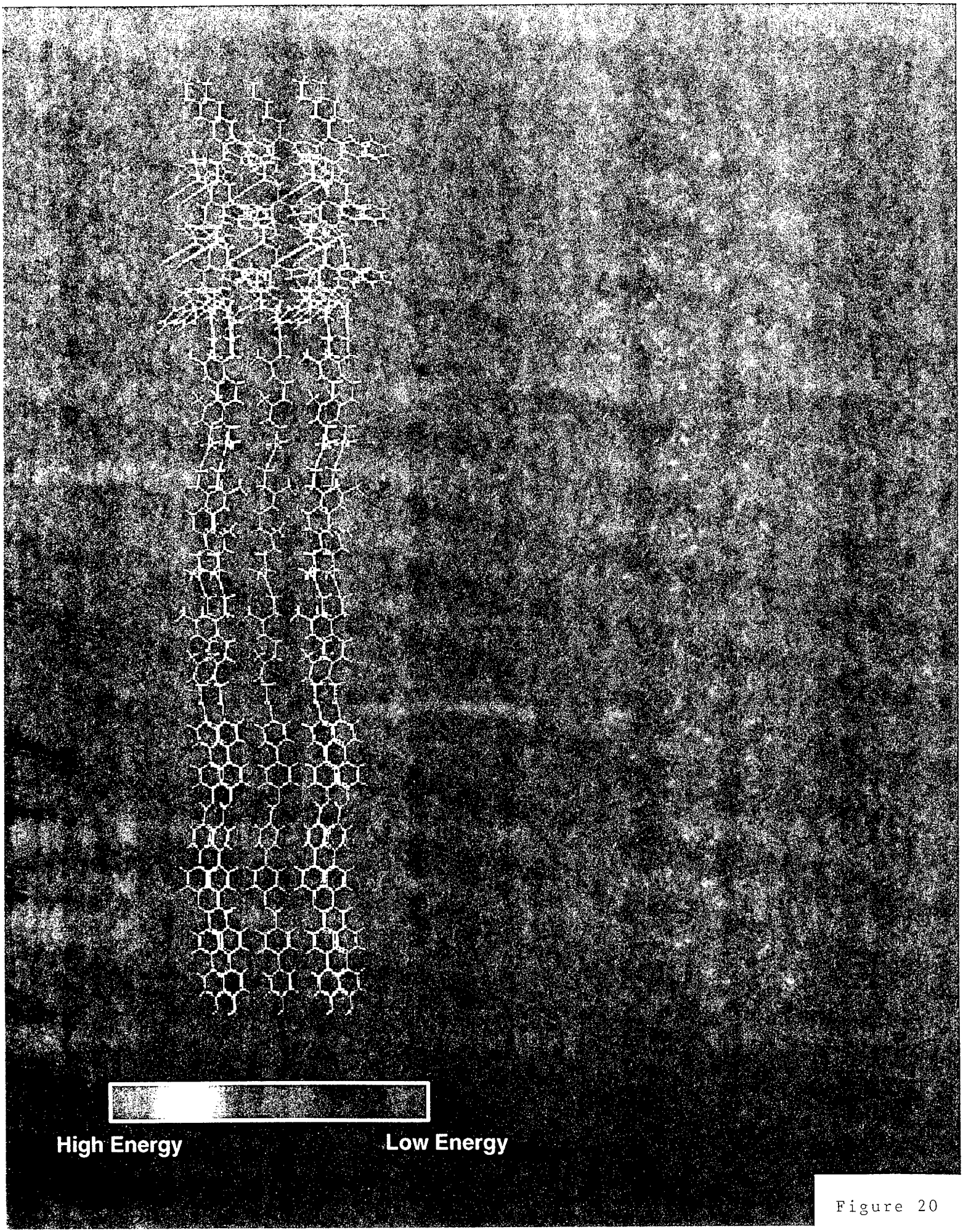

Figure 20

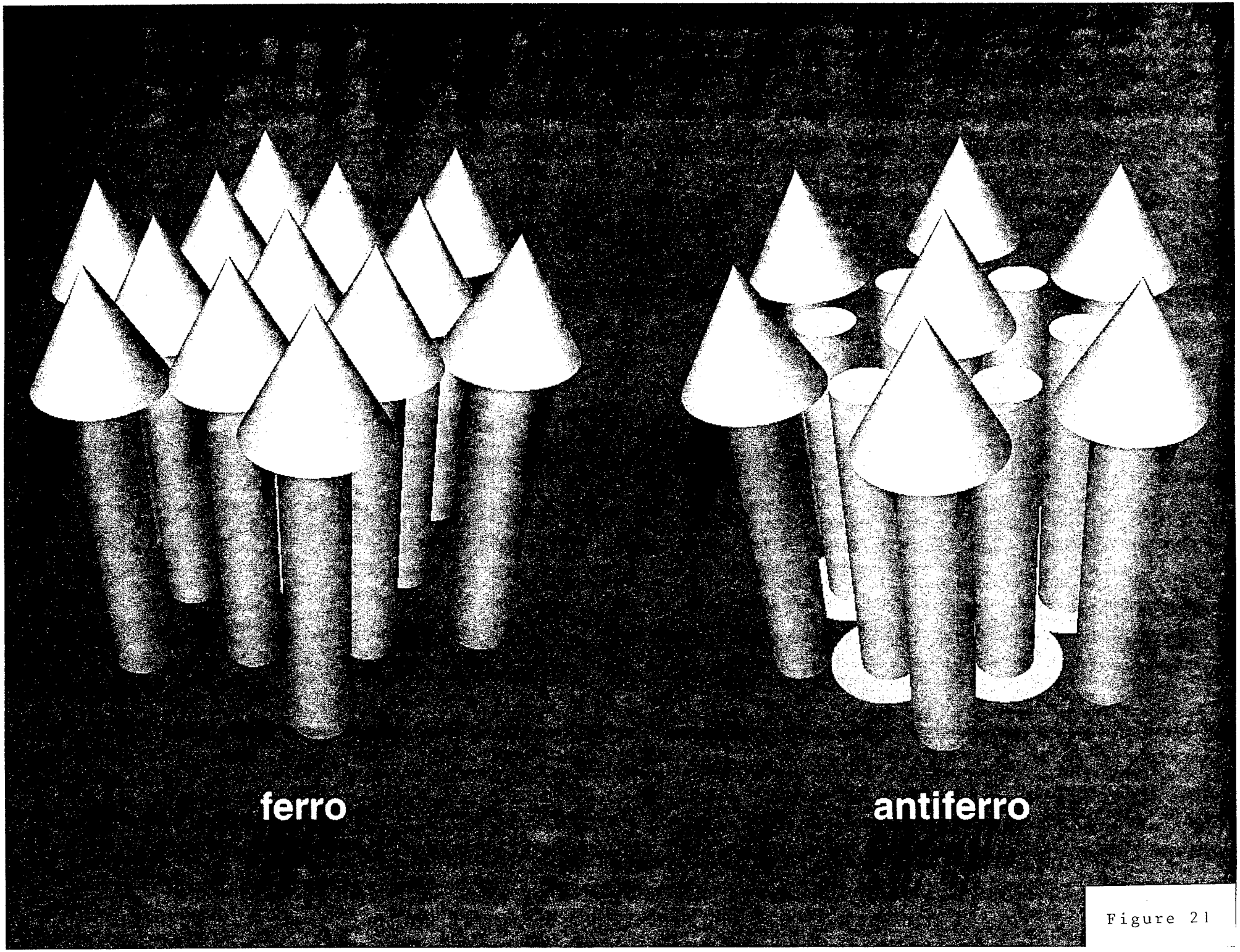

Figure 21

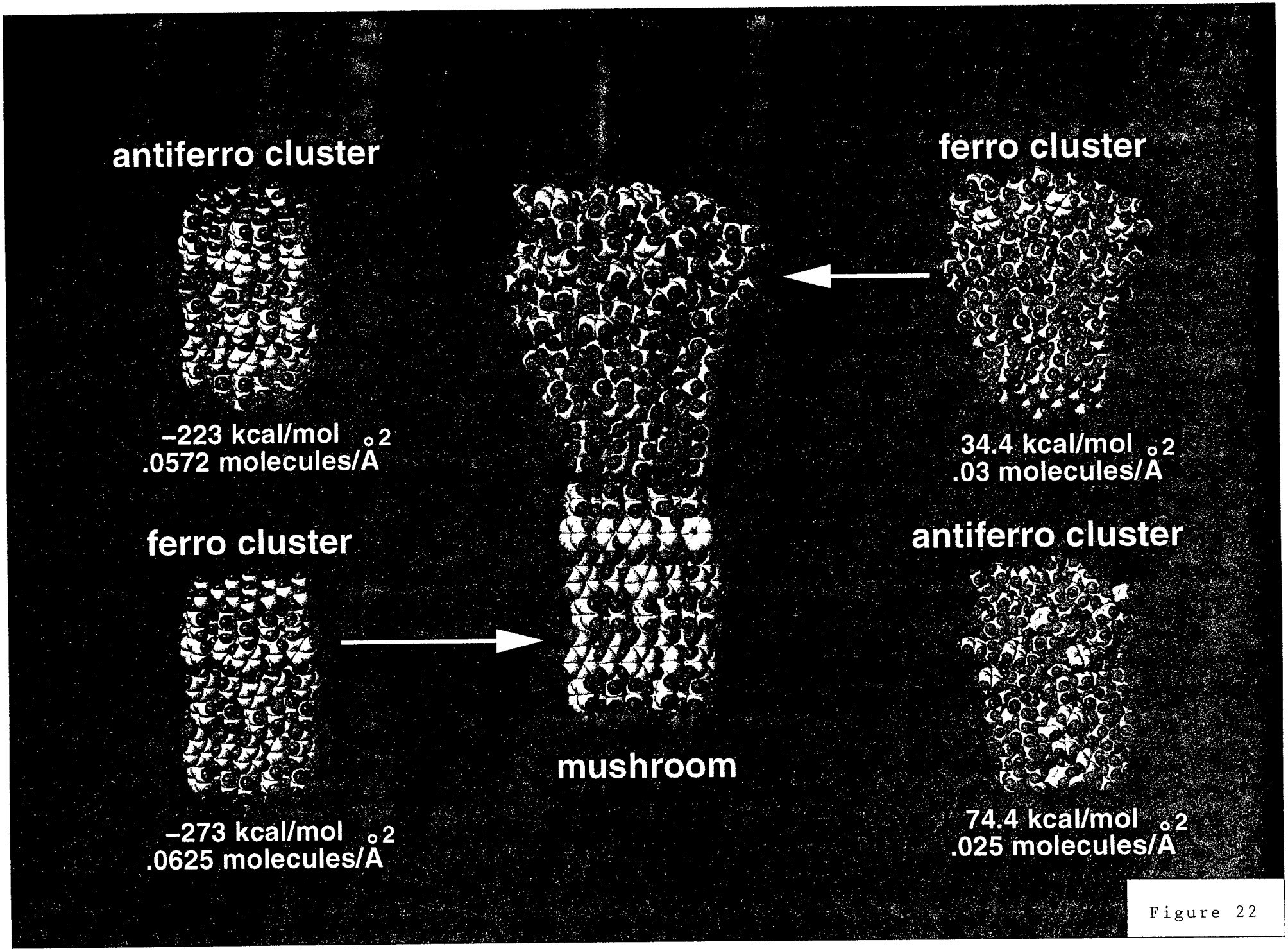
antiferro cluster
–223 kcal/mol °2
.0572 molecules/A
ferro cluster
34.4 kcal/mol °2
.03 molecules/A
ferro cluster
–273 kcal/mol °2
.0625 molecules/A
mushroom
antiferro cluster
74.4 kcal/mol °2
.025 molecules/A

Figure 22

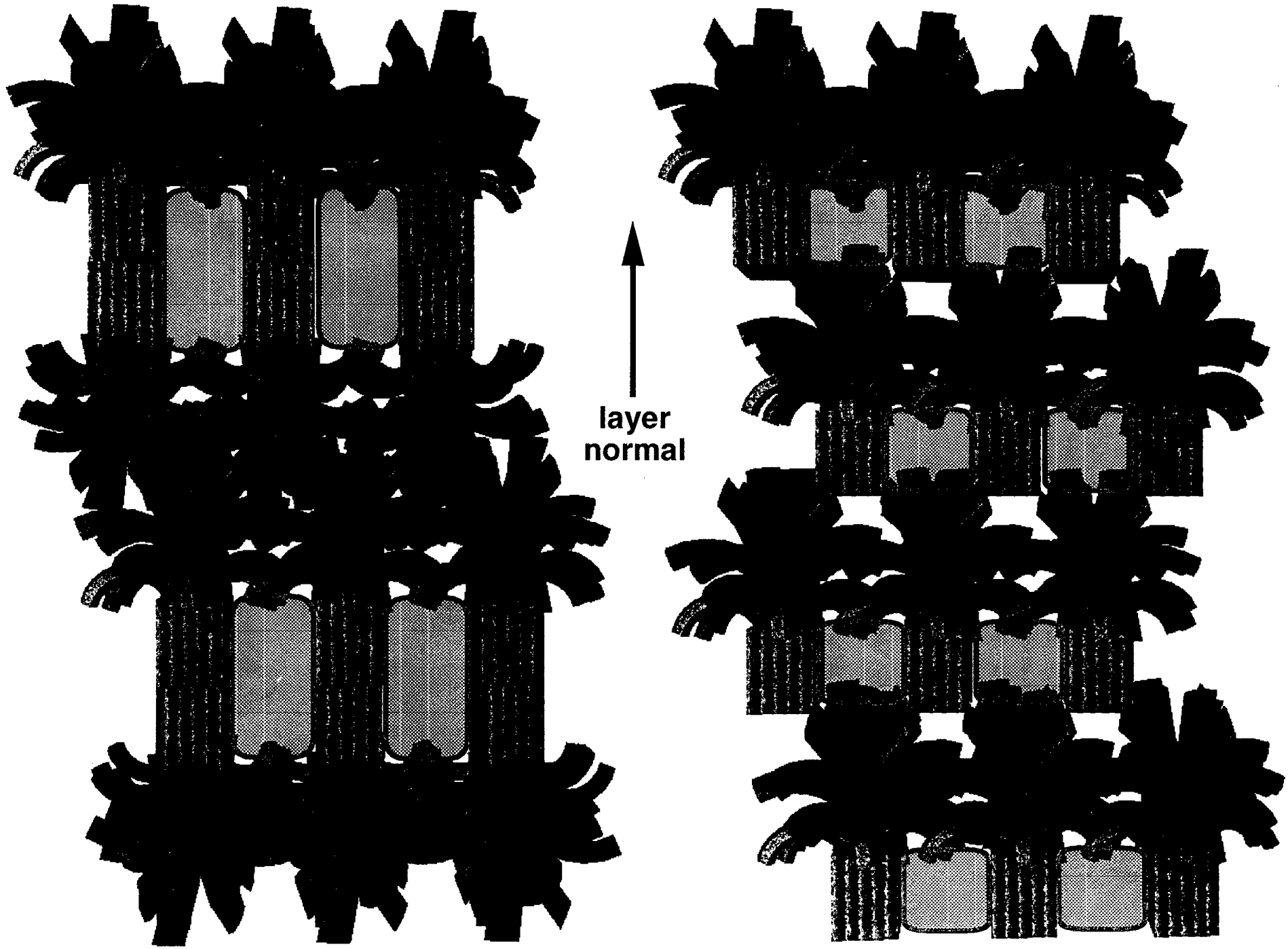

Figure 23